Spring 2009

Classification of fine particles using a Taylor-Couette device

Navina Durgaiah Tungapindi

Department:

CLASSIFICATION OF FINE PARTICLES USING A TAYLOR-COUETTE DEVICE

by

NAVINA TUNGAPINDI

A THESIS

Presented to the Faculty of the Graduate School of the

MISSOURI UNIVERSITY OF SCIENCE AND TECHNOLOGY

In Partial Fulfillment of the Requirements for the Degree

MASTER OF SCIENCE IN CHEMICAL ENGINEERING

2009

Approved by

Kimberly H. Henthorn, Advisor
Douglas K. Ludlow
Cesar Mendoza

ABSTRACT

The study of fine particle classification is common, especially since a well-defined particle size distribution is important in most processes and products. Many methods have been developed to classify micron-size particles, and although each has its own advantage, most cannot classify particles to an extremely narrow range. This is partly due to the cohesive nature of fine particles, which can be due to electrostatic attraction, moisture, or van der Waals forces. In order to overcome this problem, a wet method of classification has been chosen here. Taylor vortices, discovered in 1923, develop in the fluid contained in the annulus of two concentric rotating cylinders. It has been shown in recent years that Taylor vortices can be used to classify particles regardless of their size (which may range from a few microns to millimeters) and density difference between the particles and fluid. This method also allows for a semi-continuous throughput of particles. The present work outlines the use of Taylor vortices to classify fine particles to a narrower size distribution. The main objective here is to determine the parameters affecting classification of glass spheres of various initial distributions. Factors such as rotational velocity, system annulus size, particle to fluid density ratio, and particle feed rate have been investigated. The results obtained showed that both rotational velocity and particle feed rate have a significant effect on classification while classification for particles of size 10 μm or less was not feasible for the experimental parameter range studied here. The conclusions were supported both numerically and experimentally.

ACKNOWLEDGMENTS

I would like to express my sincere gratitude and appreciation to my advisor Dr. Kimberly Henthorn for her continued guidance, support and encouragement throughout my work. I am extremely grateful to her for making my curriculum and research a valuable learning experience. She has been a great source of inspiration and motivation during the research program and preparation of this thesis. I would also like to thank Dr. Ludlow and Dr. Mendoza, my committee members, for the support and help they have provided during my Masters degree program.

I would like to thank Mr. Dean Lenz, our lab technician, for all of his invaluable efforts in the project. Special thanks go to FLUENT technical support Kapil Das Sahu and Nidhesh Jain. I would like to thank my lab mates and friends Shanti, Annu, Mihir, and Gautham for all their help during my research.

At the top of my list are the most important people in my life: my parents. They constantly encouraged, guided and supported me throughout my life and helped me face challenges successfully. I thank my brother and also my best friend Tejaswi who has always been there for me. Special thanks also go to my close friends Kafeel, Moha, Kamakshi, and Aayushman.

Finally, I would like to thank all my friends and people who have been there for me throughout my research program and made my stay at MS&T a pleasant one.

TABLE OF CONTENTS

LIST OF ILLUSTRATIONS

Figure Page

1. INTRODUCTION

The study of fine particle classification is common, especially since a well-defined particle size distribution is important in most processes and products. Many methods have been developed to classify micron-size particles, and although each has its own advantage, most cannot classify particles to an extremely narrow range. This is partly due to the cohesive nature of fine particles, which can be due to electrostatic attraction, moisture, or van der Waals forces. The current work outlines the use of Taylor vortices to classify fine particles to a narrow size distribution.

Taylor vortices, discovered in 1923, develop in the fluid contained in the annulus of two concentric rotating cylinders [1]. The development and use of these vortices are highly researched areas. Recent work outlined by Ohmura *et al.* [2] shows that Taylor vortices can be used to classify particles regardless of their size (which may range from a few microns to millimeters) and even with a small density difference between particles and fluid. This method also allows for a semi-continuous throughput of particles. A few factors affecting classification efficiency, specifically particle properties and feed rate, and system rotational velocity and dimensions, have been studied here in order to improve the efficiency of the process.

1.1. OBJECTIVES

The main objective of this work was to classify a wide range of particles into a narrower distribution. Effects of particle properties, system rotational velocity, system annulus size, and particle feed rate on the system classification efficiency were assessed

experimentally. The effect of system rotational velocity and particle properties on classification efficiency was also studied numerically to verify the experimental trends.

1.2. BACKGROUND

1.2.1. Methods of Particle Classification. Classification, also known as grading, is usually employed to achieve a uniform distribution of particles from a mix of a wider distribution. There are many methods available for classifying particles based on their size, shape, surface roughness, density, color, and magnetic nature. Some of the common methods used in particle classification include the use of sieves, cyclone separators, electrostatic precipitators, fluidized beds in series, sedimentation, and elutriators. These methods can be broadly organized into wet and dry methods of classification (Figure 1.1).

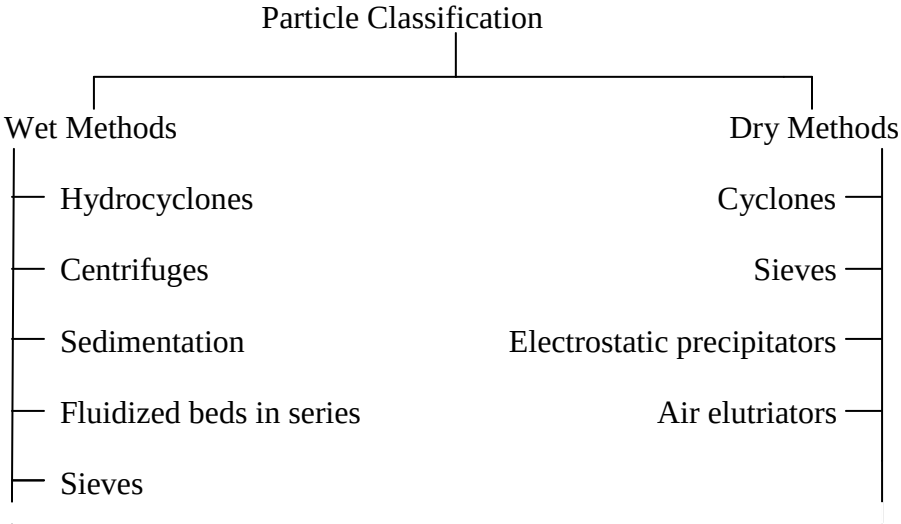

Figure 1.1. Particle classification methods

As the name suggests, wet methods of classification utilize a liquid to classify particles. Dry methods of classification usually involve either compressed air or gravity as the classification factors. As the size of the particles decreases, it is difficult to employ dry methods of classification because of increase in interparticle forces and particle-particle interactions. To avoid this, wet methods of classification are generally preferred when classifying fine particles.

1.2.1.1 Sieves. Sieves are the cheapest and most commonly used devices for classifying particles. Sieves are mechanical screens, and depending on the number of particle fractions required, more than one size of sieve may be used. Usually, a set of sieves in descending order of screen openings are stacked and the mixture of particles is poured into the top and the particles are classified into various size ranges. Gravitational force along with gyration, shaking, or vibration is instrumental in the classification process [3].

Sieving can be operated under both dry and wet conditions depending upon the nature of the particles being classified. Despite the fact that sieving (both wet and dry) is a relatively cheaper option, it is difficult to classify particles less than 40 μm using sieves because interparticle forces are prominent and the material can become extremely cohesive. In recent years, electroformed micromeshes (which can classify particles down to 1 μm) have been invented to overcome this problem [4], but their cost is very high. Additionally, aggregation is a common occurrence with wet sieving.

1.2.1.2 Cyclones and hydrocyclones. When smaller particles undergo gravitational settling, the rate of settling is small and in order to increase this rate, external forces such as centrifugal forces can be used. Cyclone separators use this

principle of centrifugal settling to classify particles and can be conducted under either dry (cyclone) or wet (hydrocyclone) conditions. Particle-laden fluid enters tangentially from the top at a high velocity, and following a spiral path along the wall of the vessel, forms a vortex. The larger particles immediately hit the wall and are separated quickly from the mix. The lighter particles and fluid exit from the top of the vessel in an inner vortex. In order to achieve complete solids removal, more than one cyclone separator can be used. Cyclones generally have a higher rate of efficiency and lower maintenance costs than most other classification methods but as particle size decreases, the efficiency drops [3]. In addition, both cyclones and hydrocyclones promote particle attrition and aggregation and typically have high operating costs to overcome the pressure drop [5].

1.2.1.3 Electrostatic precipitators. Invented in the earlier part of the 20th century, electrostatic precipitators (ESPs) are highly efficient particle classifiers that use electrostatic charge to classify particles. Gas (usually air) laden with the particles to be classified is passed through the ESP in which an electric field is created. The particles are ionized and collected on an oppositely charged plate and removed. ESPs can also be used in the wet mode by spraying the incoming particle stream with moisture. This helps to classify very fine particles and also increases the process efficiency by reducing the electrical resistance. Though ESPs have relatively high particulate removal efficiency, they are typically used to separate particles less than 5 µm in size because it is difficult to effectively charge large particles [5]. Moreover, ESPs tend to promote particle aggregation and although they have less maintenance and operating costs with lower energy maintenance, their initial capital costs are very high. In addition, ESPs do not allow flexibility of operation despite the fact that they can handle large volumes of

mixtures with low pressure drop [6]. ESPs are also not very useful for particles with high electrical resistivity.

1.2.1.4 Sedimentation. Batch sedimentation is one of the oldest and most widely known wet methods of particle classification. In this method, particles to be classified are mixed in a suspension and allowed to settle. Gravitational force plays the classifying factor in sedimentation, with the particles settling down in layers according to their size. The largest particles are found in the lower layers while the smaller ones are situated near the top. Despite being advantageous in that the particles settle according to their size, the main drawback of sedimentation is that the settled particles cannot be separated easily.

1.2.1.5 Air elutriators. Air elutriation is a process in which particles are classified by being injected into a stream of air that is flowing at a high velocity. When a mix of particles is introduced in the elutriator, the larger particles settle downward while the smaller ones are carried out upward with the operating fluid. The velocity at which air is flowing is adjusted based upon the sizes of particles present in the initial mixture, thus ensuring that the larger particles are not washed out of the elutriator along with the smaller ones. This method is primarily used with particles having a large difference in their sizes. Typically, particles larger than 10 μm can be classified using elutriation. In many industrial processes, the process of elutriation is typically followed by another mechanical separator (mostly cyclone separators) to remove the fine particulate material. Elutriator efficiency increases with increasing particle size and decreasing fluid velocity, thereby rendering it ineffective in the case of classifying smaller particles [7].

1.2.1.6 Fluidized beds in series. The use of fluidized beds in series is a recent method developed for fine particle classification. It uses the principle of hydrosizing in

which particles are hydraulically classified based on their settling velocities [8]. A wet method, it has been put to use in classifying particles up to 10 µm in size. Particles are fed into an upward flowing liquid stream and particles with settling velocities greater than the velocity of the fluid settle downward and those with smaller settling velocities are washed out with the fluid stream. This method is advantageous because it avoids particle attrition and has also proved to be better for classifying particles with narrow differences in size. Despite these advantages, since the entire process relies on gravitational force for separation, it is a time-consuming process, and its efficiency is not very high.

1.2.1.7 Centrifuges. Centrifuges use the principle of filtration for particle classification. The operation of centrifuges is similar to cyclones, where centrifugal force plays an important role in the classification. The particles are fed into a rotating drum in slurry form and under the influence of centrifugal force the particles are classified and collected in cake form on a filter. The particles settle according to their size, but once again the problem of separating them from the cake becomes an issue. Centrifugal classification of particles additionally promotes agglomeration of particles along with the occurrence of attrition.

Despite the fact that all these methods have been or are being currently employed in classifying particles, most of them cannot classify particle populations with an initially narrow size distribution. Moreover all the processes either show low efficiency in classifying small particles or promote particle attrition or agglomeration. Hence a new method is required which avoids all these disadvantages.

1.2.2. Taylor Vortices. The interaction of particles and fluid is especially important in wet methods of particle classification for process optimization. In recent years, the application of fluid instabilities for particle classification has been an increasingly popular phenomenon. Among the instabilities used for this application are Taylor vortices [2], which take the form of regularly spaced toroidal vortices in the annulus of concentric rotating cylinders (Figure 1.2) [9]. These were first discovered during an investigation into the stability of viscous liquids between two concentric rotating cylinders [1] (Figure 1.3) and it was observed that a pattern of stacked vortices formed as the flow progressed. It was explained that these were a result of instabilities formed in the fluid and experiments were conducted to identify the various conditions under which these instabilities are formed.

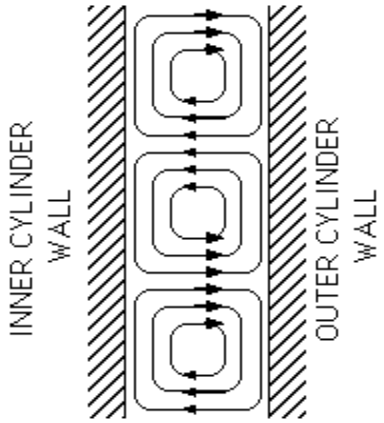

Figure 1.2. Cross-sectional view of Taylor vortices [10]

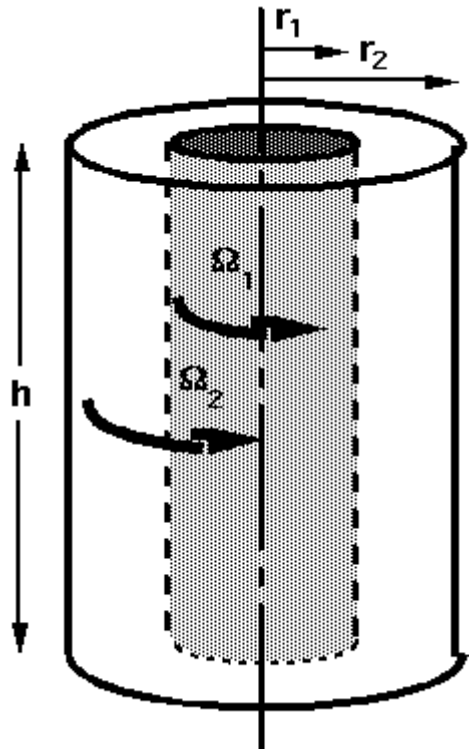

Figure 1.3. Schematic of the Taylor-Couette system [11]

In most studies, these vortices have been observed to form with only the rotation of the inner cylinder or rotation of both the inner and the outer cylinders. This phenomenon was not noticed with the rotation of outer cylinder and was proved in the work done by Couette in 1932 [1]. Couette's work showed that vortex formation is not possible even at higher rotational speeds of the outer cylinder and the flow remained circular. This circular flow was named Couette flow and is laminar by nature. When the rotational speed of the inner cylinder reaches a critical value, the laminar Couette flow becomes unstable and transitions into a cellular vortex flow called Taylor vortex flow

[12] which is turbulent in nature. The critical speed of the inner cylinder is normally defined to be when the Taylor number, Ta, is 1708 [13]:

$$Ta = 4\frac{(\Omega_1 r_1^2 - \Omega_2 r_2^2)\Omega_1 (r_2 - r_1)^4}{(r_2^2 - r_1^2)\nu} \tag{1.1}$$

The study of Taylor vortices is a highly researched area with applications in diverse areas such as heat transfer, particle classification, and magnetic applications. In recent years, particle classification has been an application of Taylor vortices. Axial Taylor vortex classification of polymethyl methacrylate (PMMA) particles (10-80 μm) in glycerin was previously examined by Ohmura *et al.* [2]. They based their investigations on the work done by Ookawara *et al.* [14], who used Dean vortices to demonstrate particle classification using fluid instabilities. Ohmura *et al.* concluded experimentally and numerically that particles from a few microns to a few millimeters in size can be classified using Taylor vortices and that despite a very small density difference (ratio of particle density to fluid density of approximately 1.04), the particles were easily classified. Ohmura *et al.* also discussed the mechanism of particle classification in a Taylor-Couette device and concluded that particles are classified axially. The larger particles bypass the vortices due to centrifugal forces and shear-induced particle migration and the smaller particles are trapped in the vortices.

The wide range of possible particle sizes can be attributed to the fact that the vorticity of the secondary vortices can be controlled with the manipulation of the rotational speed of the inner cylinder. Since larger particles bypass the vortices, millimeter-sized particles can be classified if the inner cylinder rotates at a very high speed, and if the operation occurs at a lower speed, micron-sized particles can be

classified in the same device. The above conclusions were based on the experimental classification of 10-80 µm PMMA particles with a wide initial particle size distribution. Moreover, Ohmura *et al.,* found via numerical simulation (with the commercial Computational Fluid Dynamics code Rflow©) that Taylor vortices can be used to classify particles.

Their experimental results supported the conclusions drawn from the simulations, with the majority of the small particles concentrated in the vortex core region and the larger particles situated in the outer region of the vortices. Although they studied the classification of particles in the micron range, their work did not cover particles with an initial narrow PSD. Ohmura *et al.* [2] showed both experimentally and numerically the segregation of particles into two different regions – the vortex core region and the outer region of the vortices.

1.2.3. Particle Behavior in Taylor Vortex Flow. The behavior of a particle flowing in a Taylor vortex was predicted by Wereley *et al.* [15] to be oscillatory in nature. However, gravity was not taken into account for their work. Arifin *et al.* [16] conducted experiments taking gravity into consideration and observed that particles exhibit a toroidal motion in the Taylor vortex. The particles oscillated periodically in both axial and radial directions while travelling around the vortices. Arifin *et al.* predicted that a particle accelerates while moving towards the inner cylinder and decelerates when moving near the outer cylinder. Their work also proved that when the rotational speed of the inner cylinder is reduced, the toroidal behavior is not prominent with the particles following an azimuthal trajectory.

Using CFD, a second discrete phase dispersed in a continuous phase can be modeled with the help of a Lagrangian frame of reference. The trajectories and heat and mass transfer from the discrete phase can be calculated and modeled. Various types of particle behavior such as collision, combustion, heat and mass transfer, and evaporation of liquid droplets can also be modeled. Using the discrete phase model (DPM), physical properties of inert particles such as type of material, density, and size are defined for modeling. The particle tracking equation is obtained by the integration of the force balance on the particle [17]:

$$\frac{du_p}{dt} = F_D(u - u_p) + \frac{g(\rho_p - \rho)}{\rho_p} \tag{1.2}$$

where, F_D is the drag force, u_p and u are particle and fluid velocity, g is the gravitational constant and ρ_p and ρ are particle and fluid densities, respectively.

The boundary conditions typically used while modeling particle flows are particle reflection from a boundary by elastic or an inelastic collision, particle trapped at a wall (usually evaporating/combusting particles), particle escaping (vanishing at the boundary) (Figure 1.4), particle passing through an internal boundary, and particle sliding along a wall.

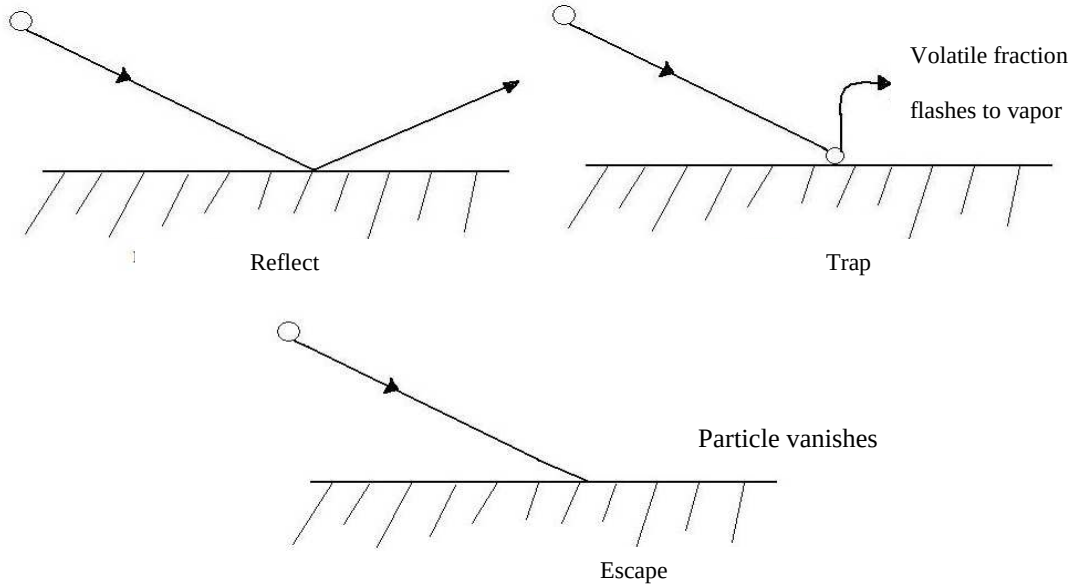

Figure 1.4. Various boundary conditions of DPM [18]

2. EXPERIMENTAL WORK

2.1. PARTICLE MATERIAL

Initial experiments were conducted using soda lime glass spheres (specific gravity= 2.5) from Mo-Sci. Corp., Rolla, MO. For qualitative purposes, these particles ranged from 10-30 µm in size. Further experiments were also conducted using soda lime glass spheres with sizes ranging from 50-120 µm and 0.1-10.0 µm. Figure 2.1 shows the particle size distribution (PSD) of the initial feeds.

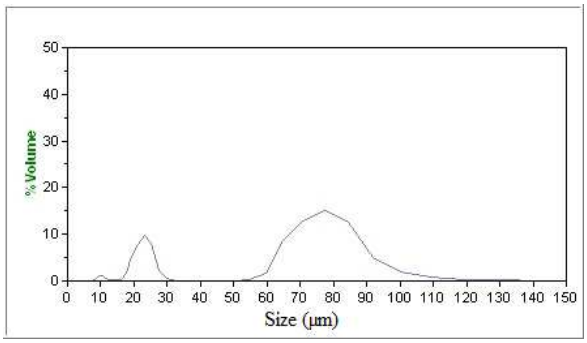

(a)

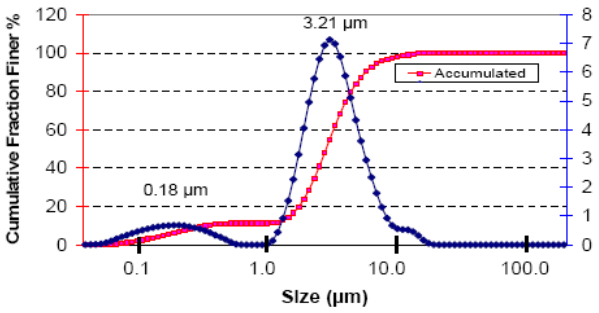

(b)

Figure 2.1. PSD of glass particles in the initial feed: (a) Size range 10-30 µm, 50-120 µm (b) Size range 0.1-10.0 µm

2.2. PARTICLE INJECTION

Glass spheres were initially formulated into a slurry with water and were poured into the system directly from a beaker, but the well-developed fluid flow was disturbed. To overcome this problem, particles were injected through a dropper, but this method was discarded as uniformity in particle feed rate was not achieved. A peristaltic pump was then used to introduce the particles in the system, which allowed for regulation of the particle feed rate and also left the developed vortex flow undisturbed.

Initially the inlet tubing of the peristaltic pump was placed in a beaker containing the particle slurry and the outlet tubing was placed in the injection port of the system. This led to very few particles being injected into the system and unsatisfactory results. To overcome this, a plug of particle slurry was introduced into the outlet tubing while the inlet tubing was placed in a beaker containing distilled water. A surfactant (Tween-80) was added to the particle slurry to prevent particle agglomeration.

2.3. EXPERIMENTAL SETUP AND PROCEDURE

The experimental set-up constructed is shown in Figure 2.2. The outer and inner cylinders were made of Plexiglas and their heights were 17 and 15 cm, respectively. The inner cylinder was coated red and the outer cylinder was transparent to allow for better observation. A funnel with the same width as that of the outer cylinder was glued to the outer system and served as a drainage port. The opening and closing of this port was controlled by a valve attached to the funnel. The inner cylinder was connected to a motor which controlled its rotational speed. An injection port was drilled into the top of the system which allowed for the introduction of the working fluid and particles.

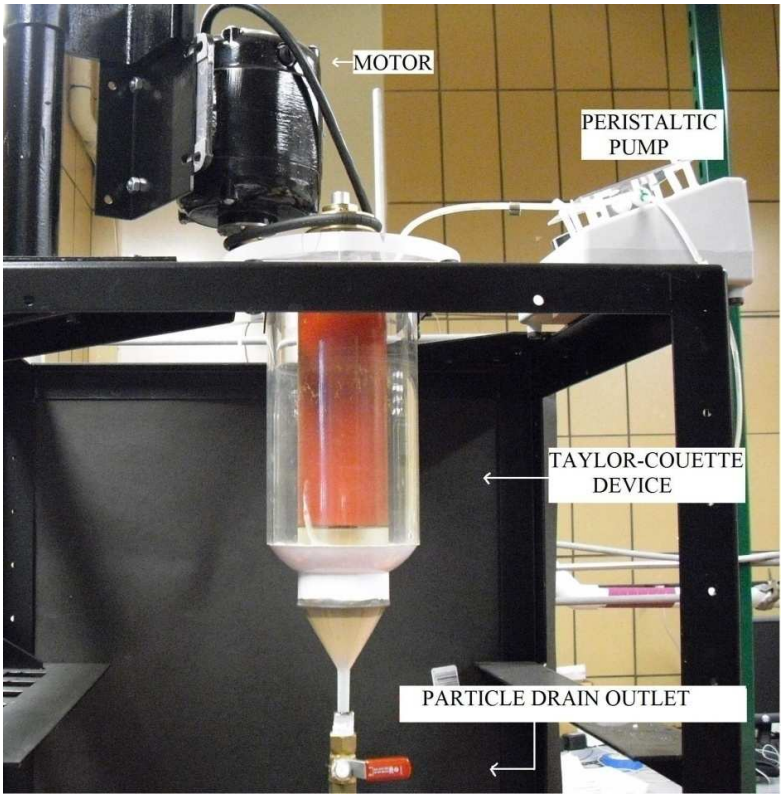

Figure 2.2. Experimental set-up

Distilled water was introduced into the system within approximately 2 inches from the injection port to avoid water spillage through the port when the system was in operation. The motor was operated at the threshold value for vortex formation and after considerable time (7-10 minutes) was allowed for the vortex stabilization, particles were introduced into the system using a peristaltic pump. Allowing sufficient time for particle classification (10 minutes), samples were collected at regular intervals from the bottom of the system for analysis. The PSD analysis of each sample was performed using a Microtrac S3500, which uses principles of laser diffraction for particle size measurement.

3. MODELING USING CFD

Taylor vortices are a form of turbulence that occurs in the annulus of two concentric rotating cylinders when the inertial or centrifugal forces dominate over the viscous forces. Many theoretical models have been developed to describe Taylor vortex flow, with each model having its own set of assumptions ranging from the narrow gap approximation [19] to periodic disturbances [20] to the basic assumption of stability of a fluid particle [21]. However, the basis for all these methods is solving the Navier-Stokes set of equations under the turbulent flow regime using various boundary approximations. This section gives a brief description of modeling turbulence and particle flow using Computational Fluid Dynamics (CFD).

3.1. COMPUTATIONAL FLUID DYNAMICS (CFD)

Developed in the early 1950s, CFD is a process of solving the basic governing equations of fluid flow with the help of numerical methods and algorithms [22]. It is generally used to predict the behavior of fluids subject to conditions such as heat transfer, mass transfer, phase change, and chemical reaction. A virtual model of the system is created and the behavior of the system is predicted by applying the various physical and chemical conditions. It has been shown that with the help of CFD, the behavior of various real-life systems can be predicted with relative accuracy. Used by various engineering disciplines (such as the automotive [23] and chemical [24] industries), CFD has been proven to both reduce costs and optimize systems.

3.1.1. Principles of CFD. The Navier-Stokes (N-S) system of equations represents in general, the conservation of mass, momentum, and energy of all flows. In order to model any system, depending upon the conditions, the corresponding N-S equations are solved. The conservation form of the N-S system of equations, representing the governing equations of continuity, momentum, and energy is [25]:

$$\frac{\partial U}{\partial t} + \frac{\partial F_i}{\partial x_i} + \frac{\partial G_i}{\partial x_i} = B \tag{3.1}$$

where U, F_i, G_i and B are the conservation flow variables, flux variables, diffusion flux variables, and source terms, respectively. Depending upon the type of flow, the N-S set of equations are simplified by either removing one or more equation or by not including one or more terms. For a given problem, the N-S system of equations is modified using various discretization techniques. Discretization refers to the conversion of the conservation equations to a simple algebraic form where they take values from the discrete points. Three common discretization techniques are the finite difference method (FDM), finite element method (FEM), and finite volume method (FVM) [26].

3.1.2. Finite Difference Method (FDM). FDM is generally used for compressible flows. In FDM, the governing equation partial derivatives are replaced by finite different quotients which are obtained by Taylor series. A few grid points are considered on the domain and the finite difference equation is applied to the points where variable/information is not known and the boundary conditions are applied. The process values at discrete points (nodes) are obtained by forward, backward, and central differencing schemes [27]. The values obtained are used to solve the governing equations which are converted to a system of linear equations. One drawback of FDM

includes its inability to implement gradient boundary conditions accurately, requiring difficult coordinate transformations for complex geometries and not being able to ensure that conservation laws are satisfied.

3.1.3. Finite Element Method (FEM). FEM, also known as finite element analysis (FEA), is used to solve both partial differential and integral equations. FEM is adaptable for application to complex geometries and is useful for elliptical types of problems. It was primarily used in structural analysis and for simple flow problems during its conceptual stages. In FEM, the system is divided into various elements, and properties for each element are calculated by converting the governing equations. The selection of local interpolation functions is done in such a manner that continuity between adjacent elements is maintained [28]. These local functions in turn represent the global function – the modified algebraic governing equations. The main disadvantage in using FEM is that with its use, higher computational power will be required for solving CFD problems (which require a large number of discretized points for solution).

3.1.4. Finite Volume Method (FVM). In FVM, the partial differential equations of the governing equations are converted to algebraic equations. Similar to FDM, the domain is divided into sub-domains called control volumes. Each control point has a grid point where the variable is evaluated. The governing equations are integrated over the control volume and using various profiles, the integrals are approximated [22]. A set of linear equations for the problem is obtained after the discretized equations followed by boundary conditions are applied to every control volume. The advantages in using FVM are that it can be used for unstructured grids thus allowing for modeling of complex geometries without requiring coordinate transformations. Also, conservation of all the

variables is enforced across the control surfaces of the domain. There is no loss or gain of a conserved variable and the discretized governing equations retain their physical interpretation [29]. FVM is cost effective as it saves a lot of computational power by not allowing for repetition of calculations at similar surfaces. The following set of equations show the conversion of the N-S equations into their finite volume form. The N-S system of equations is:

$$R = \frac{\partial \mathrm{U}}{\partial \mathrm{t}} + \frac{\partial \mathrm{F_i}}{\partial \mathrm{x_i}} + \frac{\partial \mathrm{G_i}}{\partial \mathrm{x_i}} - \mathrm{B} \tag{3.2}$$

The finite volume equations are obtained by integrating and then summing over all the control volumes of the domain of the flow field (Ω) [22]:

$$\int_{\Omega} R d\Omega = \int_{\Omega} \left(\frac{\partial U}{\partial t} + \frac{\partial F_i}{\partial x_i} + \frac{\partial G_i}{\partial x_i} - B\right) d\Omega = 0 \tag{3.3}$$

$$\int_{\Omega} \left(\frac{\partial U}{\partial t} - B\right) d\Omega + \int_{\Gamma} (F_i + G_i) n_i d\Gamma = 0 \tag{3.4}$$

where n_i denotes the unit vector component normal to the boundary surface (Γ). Summing over all the control volumes (CV) and control surfaces (CS), we obtain equation (2.5) which is the finite volume equation of the N-S system of equations.

$$\sum_{CV} (\Delta U - \Delta t B) \Delta\Omega + \Sigma \Delta t \underset{CS}{(F_i + G_i)} n_i \Delta\Gamma = 0 \tag{3.5}$$

3.2. TURBULENT FLOW MODELING IN CFD

The turbulent flow regime is characterized by the disordered behavior of a fluid including a rapid variation of flow properties such as velocity, momentum, species

concentration, and energy. In turbulent flow, fluid particles form groups called eddies and flux (momentum, mass, volume, or heat) takes place between them. The size and shape of these eddies vary randomly in the flow. In CFD, due to the high cost involved in modeling fluctuating properties, the time-averaged equations of the instantaneous governing equations are used to model incompressible flows [30]. Turbulent flow properties are usually written in the form

$$\phi = \overline{\phi} + \phi' \tag{3.6}$$

where ϕ, $\overline{\phi}$ and ϕ' are the instantaneous, mean, and fluctuating properties. The variation of the mean properties and the effect of the fluctuating components are considered in turbulent flow modeling. The effects of the mean properties and not the instantaneous properties are studied in turbulent modeling [22]. Several turbulent models are commonly used, including the Boussinesq approximation, Cebeci – Smith model, Baldwin – Lomax model, Baldwin – Barth model, Spalart-Allmaras model, k-ε and k-ω models, v^2-f model, Reynolds stress model (RSM), detached eddy simulation (DES) model, and large eddy simulation (LES) model. These models differ in the amount of physics involved and the degree of accuracy.

One of the most widely used turbulence models, the k-ε method, is based on modeling transport equations for the turbulent kinetic energy (k) and its dissipation rate (ε). Three common variations of the k–ε model are the standard k–ε, renormalization group (RNG) k–ε, and realizable k–ε models [31]. The three models have similar forms of transport equations for k and ε. However, each method differs in its way of calculating the turbulent viscosity, Prandtl number, and the generation and destruction terms for ε.

The standard k–ε model is the simplest model and allows for the easy determination of turbulent velocity and length scales. The equation for turbulent kinetic energy dissipation rate (ε) is obtained by taking the moments of the N-S equation as [32]

$$\mu_T = \frac{C_\mu \rho k^2}{\varepsilon} \tag{3.7}$$

where μ_T is the eddy viscosity, ρ is the density of fluid, and the value of the closure coefficient, C_μ, is 0.09. The equation for turbulent kinetic energy (k) is given as

$$\rho \frac{\partial k}{\partial t} + \rho \bar{U}_j \frac{\partial k}{\partial x_j} = \tau_{ij} \frac{\partial \bar{U}_i}{\partial x_j} - \rho\varepsilon + \frac{\partial}{\partial x_j}[(\mu + \mu_T/\sigma_k)\frac{\partial k}{\partial x_j}] \tag{3.8}$$

Hence, the ε equation is now obtained as

$$\rho \frac{\partial \varepsilon}{\partial t} + \bar{U}_j \frac{\partial \varepsilon}{\partial x_j} = C_{\varepsilon 1} \frac{\varepsilon}{k} \tau_{ij} \frac{\partial \bar{U}_i}{\partial x_j} - C_{\varepsilon 2} \frac{\varepsilon^2}{k} + \frac{\partial}{\partial x_j}[(\mu + \mu_T/\sigma_\varepsilon)\frac{\partial \varepsilon}{\partial x_j}] \tag{3.9}$$

where τ_{ij} is the apparent stress, $\bar{U}$ is the mean velocity, and the values of the coefficients are [32]:

$C_{\varepsilon 1} = 1.44$, $C_{\varepsilon 2} = 1.92$, $\sigma_k = 1.0$, and $\sigma_\varepsilon = 1.3$

In order to confirm the experimental results obtained, a numerical analysis was performed on the process. The use of a commercial CFD package for numerical analysis of a process can reduce the quantity of resources spent in conducting experiments for validation. Hence, FLUENT® (ANSYS®, Inc.), a commercial CFD package, and the CFD preprocessor GAMBIT® (ANSYS, Inc.) were used in the current project to model the Taylor-Couette device to perform the computational analysis.

3.3. FLUENT

FLUENT is a popular commercial CFD code that uses the finite volume method of evaluation to model and analyze a given problem. It is generally used along with preprocessors such as TGrid and GAMBIT, with the latter being more popular. FLUENT can be used to model complex systems involving transport phenomena, heat transfer, mass transfer, chemical reactions, or a combination of these. Using GAMBIT, a 2- or 3-dimensional model of the system is created and meshed using various mesh schemes (ex: triangular, quadrilateral, tetrahedral, hexahedral, pyramid, wedge, and hybrid) depending upon the geometry.

In FLUENT, the Graphical User Interface (GUI) is used to define specific system working conditions of the system. Using the GUI, working conditions and the type of flow (laminar or turbulent) can be specified, based on which the system is analyzed. Along with the operating conditions of the system, the pressure, velocity, and temperature boundary conditions can also be specified. Both steady and unsteady states along with deformable zones and single and multiple phases can be modeled using FLUENT.

In most cases, the standard options present in the GUI are adequate to evaluate the system, but sometimes they might not be sufficient. In such cases, FLUENT allows the users to input their own values for the operating conditions of the system. This is done by the User Defined Function (UDF) method where the user can specify various changes to occur in the system according to their requirements. UDFs are programs written by the user and are connected to FLUENT to specify the preferences of the user. For example,

if the temperature of a system needs to be varied at specific intervals of time, then, with the help of a UDF, FLUENT can be told to vary the temperature accordingly.

Modeling of systems involving moving parts can be done in FLUENT with varying frames of reference depending upon whether the entire system is in motion or only parts of it are. Deformable zones can be modeled using either sliding or dynamic meshes depending upon presence of relative motion between zones or change in shape of the system based on time. Multiphase modeling in FLUENT is done with the help of Volume of Fluid (VOF), Eulerian, and DPM methods, the first being employed for immiscible liquid systems and the latter two for solid-liquid systems. Once the simulation of the working of a system is complete, the results can be obtained in either graphical or report format depending upon choice of the user. The formation of the Taylor vortices in this device was simulated using versions 6.2.16 and 6.3.26 of FLUENT.

3.3.1. 3-D Modeling of Taylor Vortices. Using GAMBIT, a model of the modified Taylor-Couette device was created. In the model, the bottoms of both cylinders were tapered to allow for the easy drainage of classified particles (Figures 3.1 (a) and (b)) and an injection port was included for the system. By including these modifications in the Taylor-Couette device, the system resembled the real-life apparatus with options to both inject and remove particles from the system. The schematic shown in Figure 3.1(a) was constructed for the numerical evaluation purposes.

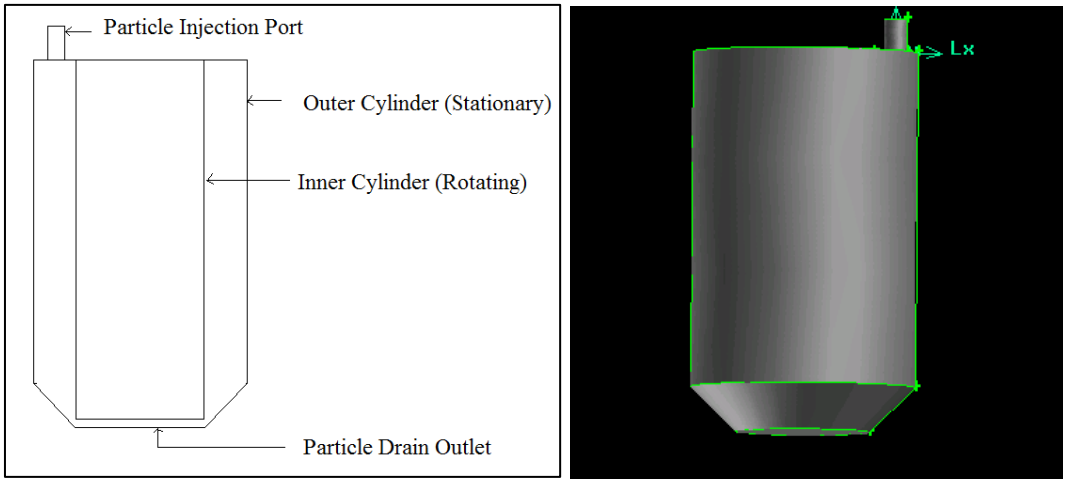

(a) (b)

Figure 3.1. Modified Taylor-Couette system: (a) Schematic (b) Computer generated model

In the model, the vertical length and diameter of the outer cylinder were 17 cm and 10 cm, respectively, and tapered near the bottom so that its smallest width was equal to the diameter of the inner cylinder. The length and diameter of the inner cylinder were 16.5 cm and 6.0 cm, respectively. The inner cylinder was shortened by 0.5 cm to allow an opening for the particles to slide down as they are classified, which allows the process to be easily converted from batch to semi-continuous operation. At the top, an injection port 2 cm high and 1 cm wide was placed in the annulus for the easy introduction of particles. This port was located equi-distant from each cylinder on the top wall of system. The model was then meshed using a tetrahedral scheme (Figure 3.2) and exported to FLUENT for further analysis.

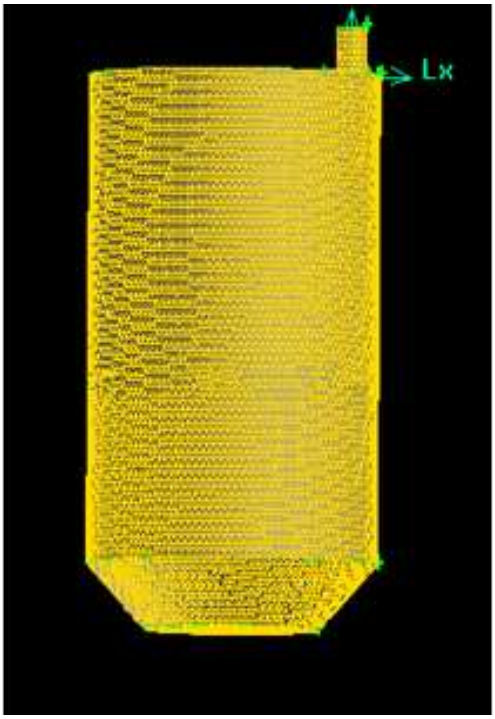

Figure 3.2. Computer-generated model of the meshed geometry

In FLUENT, the exported mesh was analyzed using the finite volume method and the standard k-ε turbulence model (with standard coefficients) was used to simulate the formation of Taylor vortices. The system was calibrated by comparing the values of normalized radial velocity at a Reynolds (Re) number of 103 to the experimental values obtained by Wereley *et al.* (Figure 4.3) [33]. For Taylor vortex flow, the Reynolds number is calculated as [34]

$$\mathrm{Re} = \frac{r_i \Omega d \rho}{\mu} \tag{3.10}$$

where, r_i is the inner cylinder radius, Ω is the rotational velocity of the inner cylinder, d is the width of the annulus, ρ is the fluid density, and μ is the fluid viscosity.

In Figure 4.3, x-coordinate, ζ, is the ratio of the axial position to the annulus size (2 cm for the current system) and the y-coordinate is the ratio of the radial velocity (v_r) at given axial location to the surface velocity of the inner cylinder, $r_i*\Omega$ (where r_i is inner cylinder radius and Ω is the rotational velocity of inner cylinder). The results obtained from the current system were in good agreement with those obtained by Wereley *et al.* as shown in Figure 3.3, validating the parameters used in the current system for modeling Taylor vortices. All the surfaces in the system (excluding the inner cylinder) were specified as stationary walls and the inner cylinder was specified as a rotating wall.

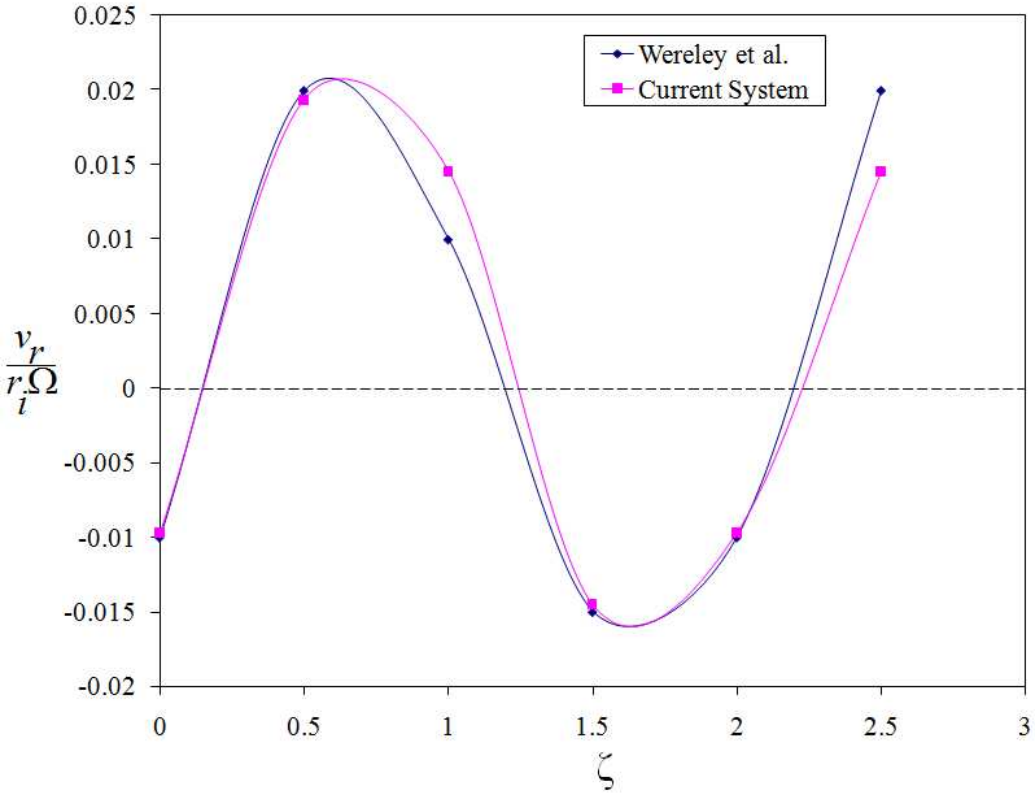

Figure 3.3. Comparison of the normalized radial velocity data (Re=103) [33]

In the simulations, water was used as a fluid and the rotational velocity of the inner cylinder was set to a threshold value of 35 rpm based upon theoretical calculations given by Equation 1.1. The Reynolds number of the system was found to be 1941, which lies in the typical Reynolds number ranges for Taylor vortex flow [34]. Figure 3.4 shows the fully developed and stabilized Taylor vortices. The solution obtained was independent of the grid and turbulence model chosen, as the values of radial velocities obtained for both the standard and realizable k- ε models were similar (Figure 3.5). The standard and realizable k- ε models were chosen as they give the best possible solution for the turbulent flows in which vortices and rotation are involved [35].

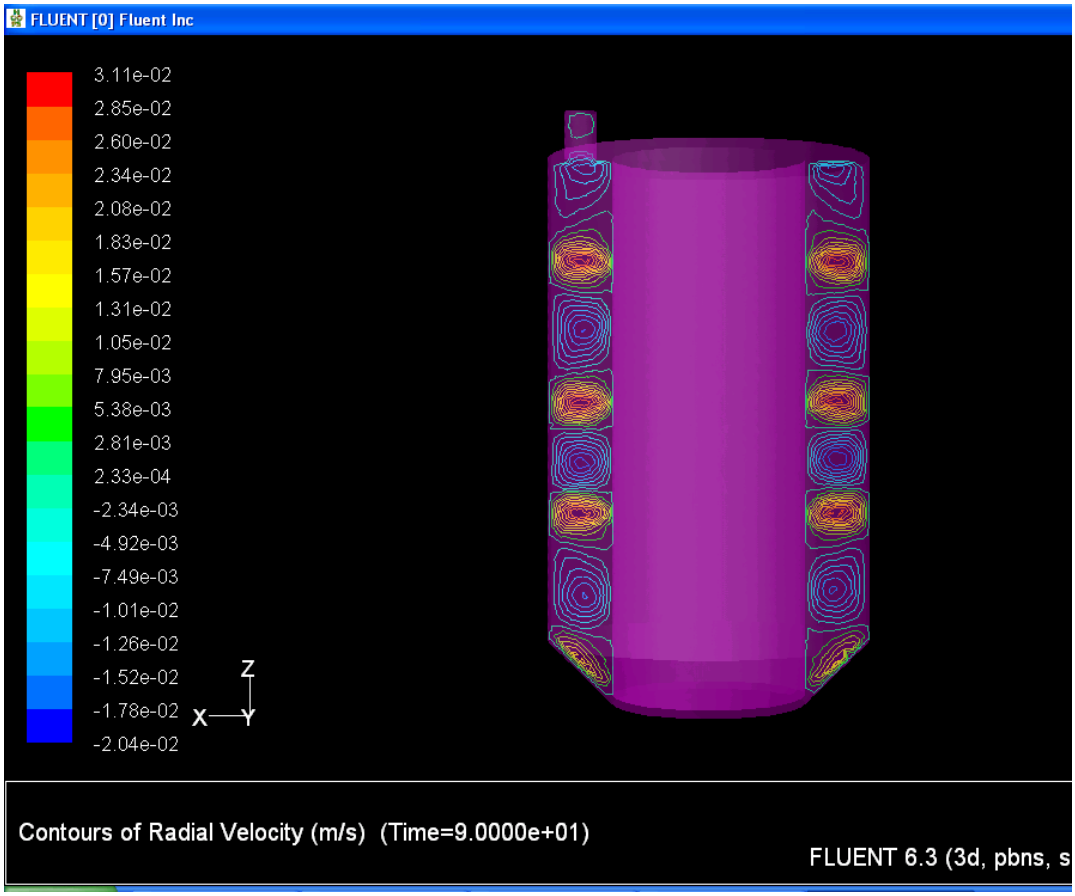

Figure 3.4. Developed Taylor vortices in the modified Taylor-Couette device

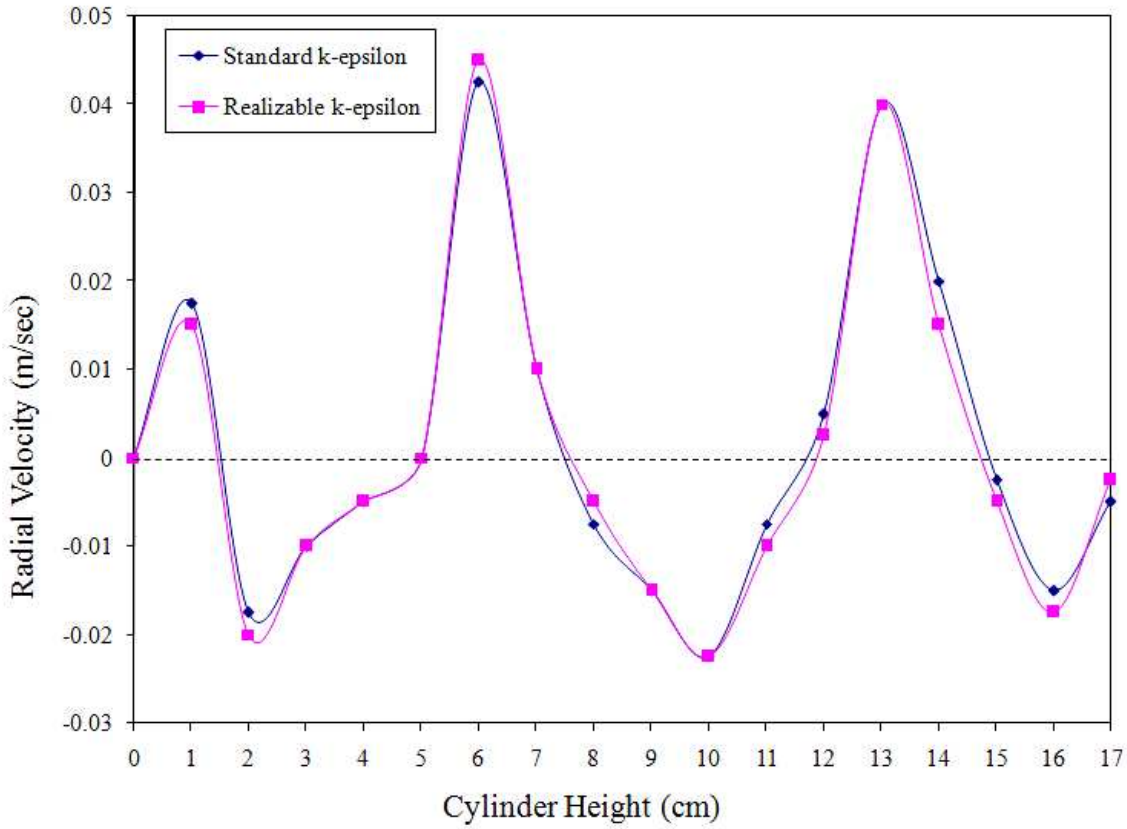

Figure 3.5. Radial velocity data of the system indicating turbulent model independency

3.3.2. Modeling Particle Flow in a Taylor-Couette Device

Once the Taylor vortices were stabilized, particles were injected into the system. Using DPM, transient or unsteady treatment of particles was performed with the particles being tracked at every fluid flow time step from the point of their injection. A transient approach was chosen since the particles were not being injected at the beginning of the flow but were being injected only after vortex stabilization. Moreover, the particles were being injected for a short period of time and not for the entire duration of the simulation.

The reflection boundary condition of the discrete phase modeling was set for all the walls in the system.

The initial conditions of the particles such as initial coordinates, velocity, diameter, material, and mass flow rate at which they were being injected were defined. Since the point properties vary with the type of injection chosen, it was essential to select the injection type before performing any simulations. The merits and demerits of the various types of injections were evaluated before the selection of a surface injection. In this type of injection, FLUENT randomly selects points on the surface (in this case, the injection port) and injects particles based upon the properties defined.

For surface injections, the initial velocity, diameter of the particles, mass flow rate at which the particles were injected, and the duration of the injection were specified. The initial positions of the particles were randomly chosen by the solver. Multiple injections of varying particle size were chosen and after all the properties were set, the flow field was initialized and the flow was simulated. The resulting particle tracks are shown in Figures 3.6 and 3.7.

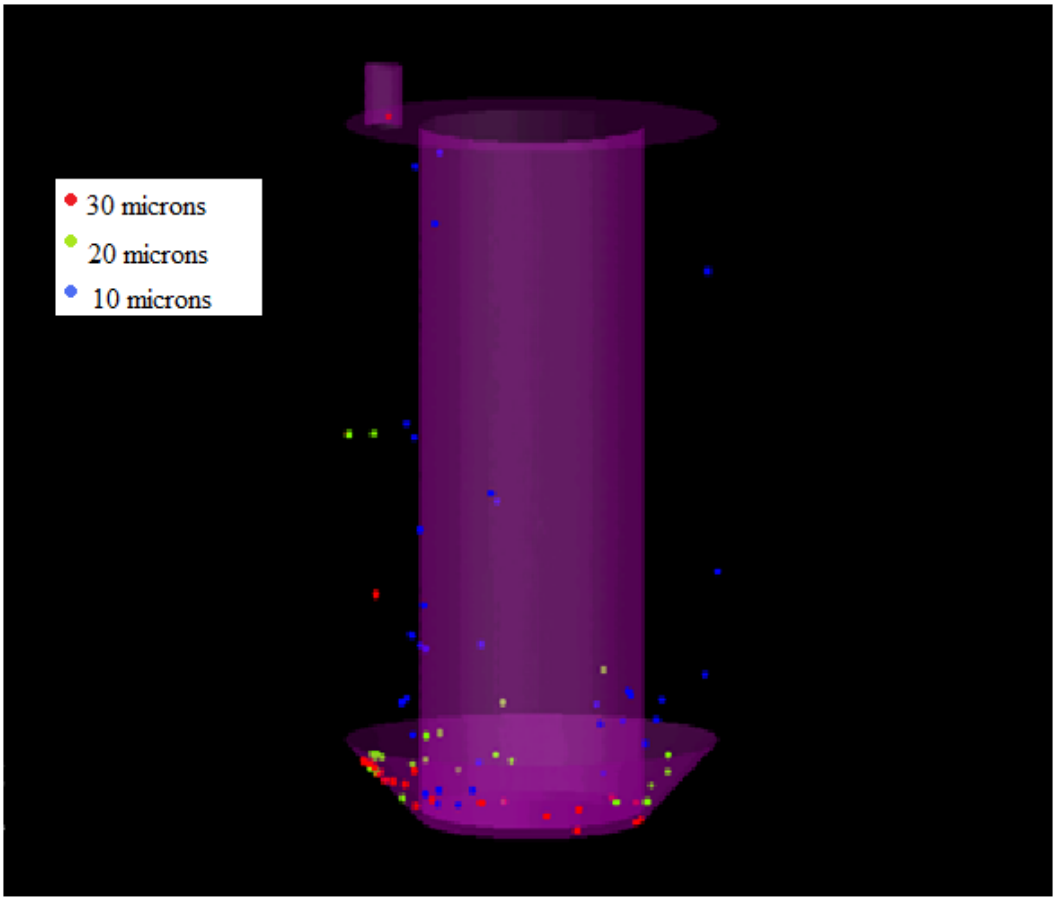

Figure 3.6. Particle tracks at the end of a simulation

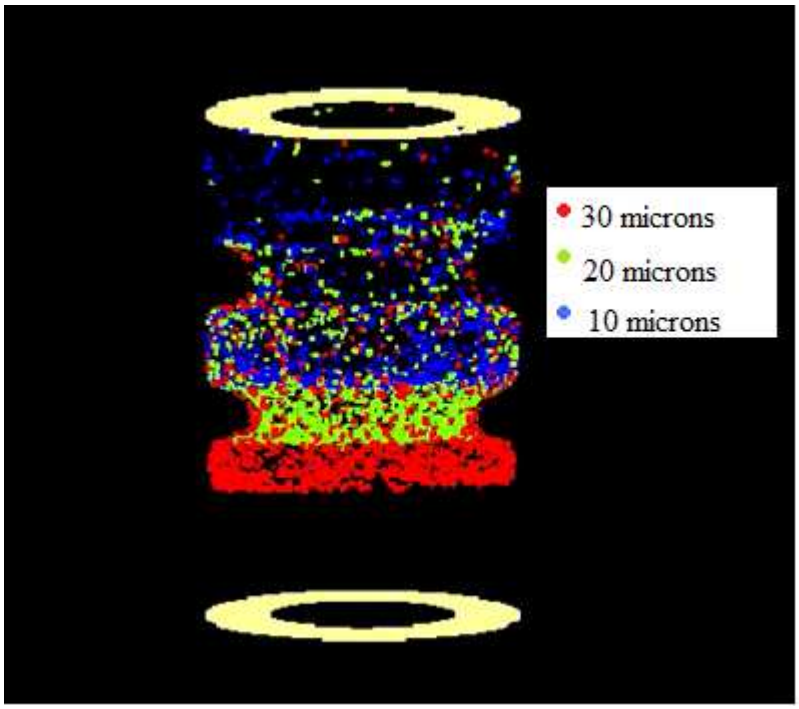

Figure 3.7. Particle tracks (t=75 s)

4. RESULTS AND DISCUSSION

4.1. INITIAL EXPERIMENTS

Initial experiments were conducted using soda-lime glass spheres to study the process feasibility. The procedure explained in Section 3.3 was followed to carry out the particle classification process. The velocity of the inner cylinder was set to a value of 35 rpm which is the threshold value for vortex formation of this system. This value was calculated from Equation 1.1, with a Taylor number of 1708. To classify particles smaller than the minimum cut-size of the current system, the inner cylinder velocity should be decreased, but if this value of velocity is lower than the threshold value, vortex formation would not be occur and no classification can take place. Therefore, the minimum cut-size was assessed by setting the velocity to the threshold value.

Water was used as the operating fluid and glass particles of size ranging from 10-110 µm were injected at a mass flow rate of 1.6 g/min once sufficient time had elapsed for vortex stabilization. Figure 4.1 shows the PSD of the initial feed and final classified product. As predicted, particles were axially classified with the amount of the smaller particles (10-30 µm) present in the final classified sample reducing significantly from an initial 10% to 5% and the amounts of the larger particles (50-110 µm) increasing from 15% to 27%. These values signify that classification has indeed taken place in the current system and the process was feasible.

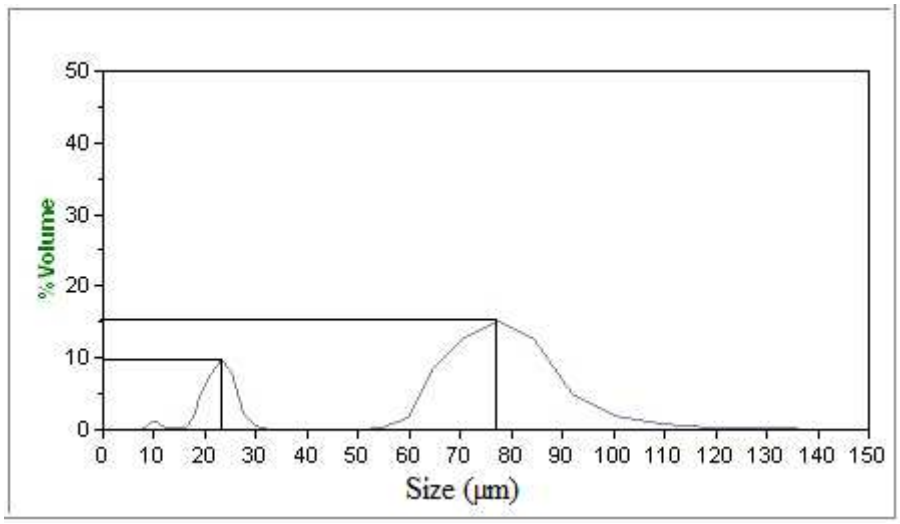

(a)

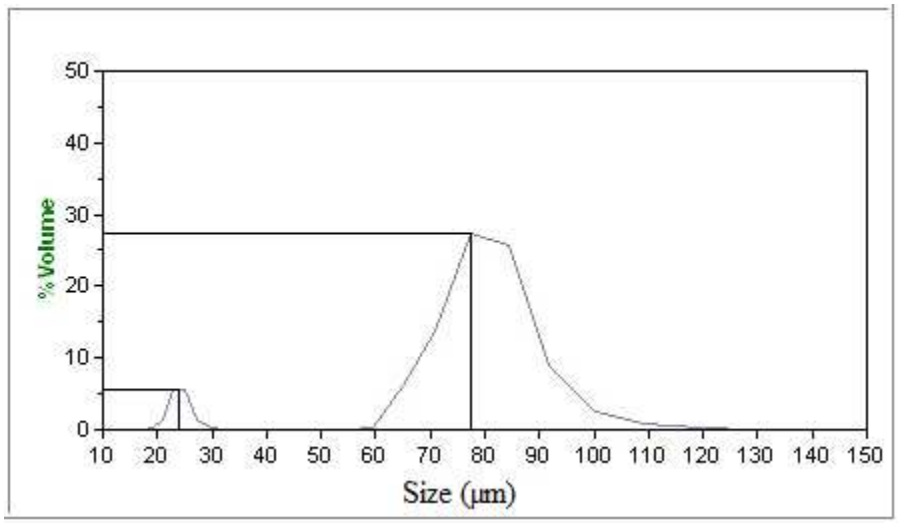

(b)

Figure 4.1. Particle size distribution of glass particles at 35 rpm inner cylinder velocity: (a) PSD of the feed (b) PSD of sample collected from bottom of the system

4.2. EFFECT OF INNER CYLINDER VELOCITY

Using soda-lime glass spheres of size range 10-30 µm, the effect of inner cylinder velocity on the classification was studied experimentally by varying the inner cylinder velocity from 35 rpm to 75 rpm (Figure 5.2). As the velocity of the inner cylinder is increased, the speed of the vortices increases, leading to an increased number of smaller particles trapped in them, allowing the larger particles to bypass the vortices. From Figure 4.2, it can be observed that as the velocity is increased from 35 rpm (Re=1941) to 75 rpm (Re=4731), the PSD curve shifts towards the right, reducing the number of smaller particles (below 20 µm) in the sample and increasing the number of larger particles (above 20 µm). It can also be observed that the maximum amount of particles present in the classified sample shifts from near 20 µm to closer to 25 µm. These values indicate that an increased separation can be achieved with an increase in inner cylinder velocity.

Experiments were also conducted for 0.1-10.0 µm particles at an inner cylinder velocity of 35 rpm to verify whether classification can be achieved for particles less than 10 µm using the current parameters. Figures 4.3 (a)-(b) show the PSD of the initial feed and the PSD of a sample collected from the bottom of the cylinder. There is no difference observed between the curves, thus signifying that no classification has taken place. Hence, classifying particles 10 µm or less is not feasible at the current experimental conditions.

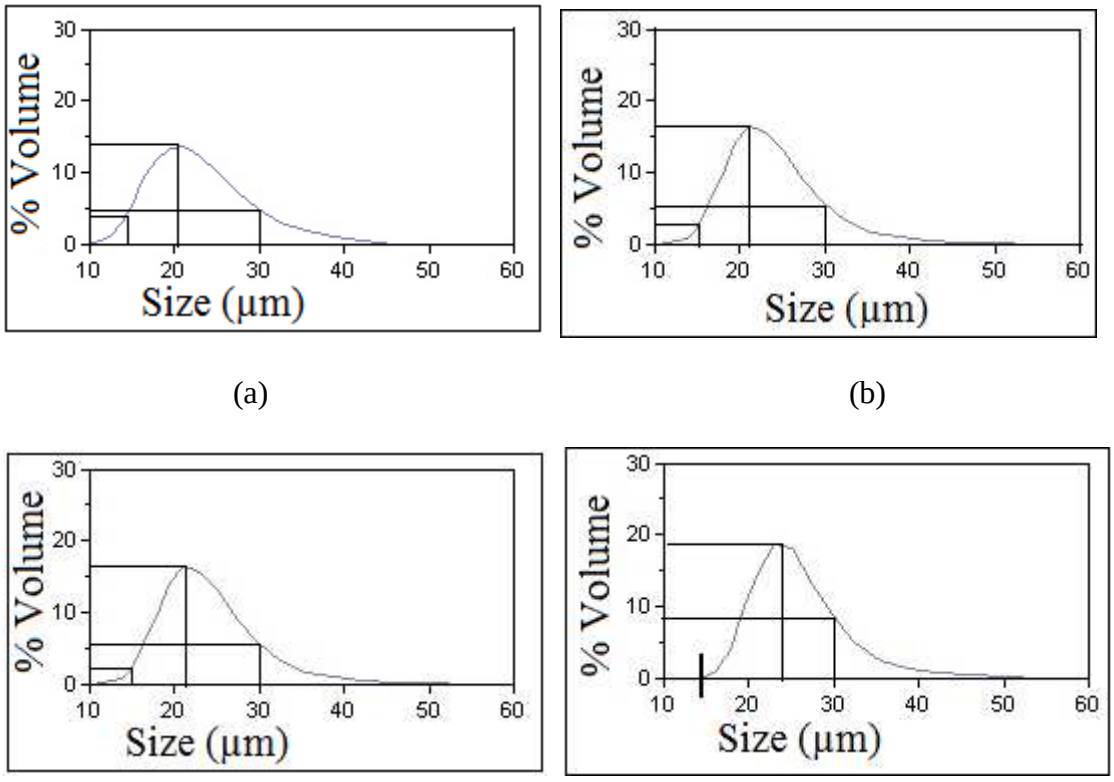

(a) (b)

(c) (d)

Figure 4.2. Effect of inner cylinder velocity on classifying glass particles (10-30 µm): (a) PSD of feed (b) PSD of bottom sample at 35 rpm (c) PSD of bottom sample at 50 rpm (d) PSD of bottom sample at 75 rpm

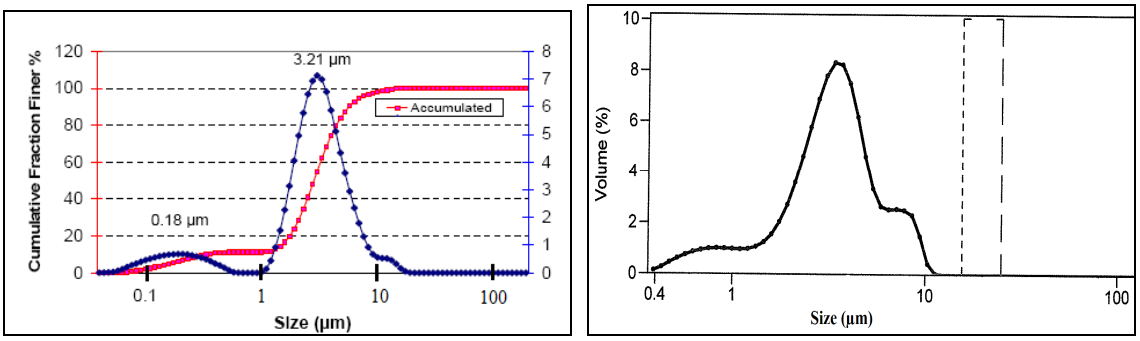

(a) (b)

Figure 4.3. Effect of inner cylinder velocity on classifying glass particles (0.1-10.0 µm): (a) PSD of feed (b) PSD of a sample collected from bottom of the system after classification (35 rpm inner cylinder velocity, steady state)

4.3. EFFECT OF PARTICLE FEED RATE

Using glass spheres of size range 10-110 µm, the effect of particle feed rate was studied experimentally by varying the inlet mass flow rate of particles from 0.8 g/min to 3.2 g/min. The data obtained is shown in Figure 4.4. The effect of particle feed rate on classification was significant; the amount of smaller particles present in samples collected from the bottom reduced from 15% at 3.2 g/min to 4% at 0.8 g/min. This behavior can be attributed to the fact that vortex formation is disturbed with the addition of particles at higher feed rates, and by the time they are stabilized, the smaller particles have travelled towards to the bottom, thus resulting in poor classification.

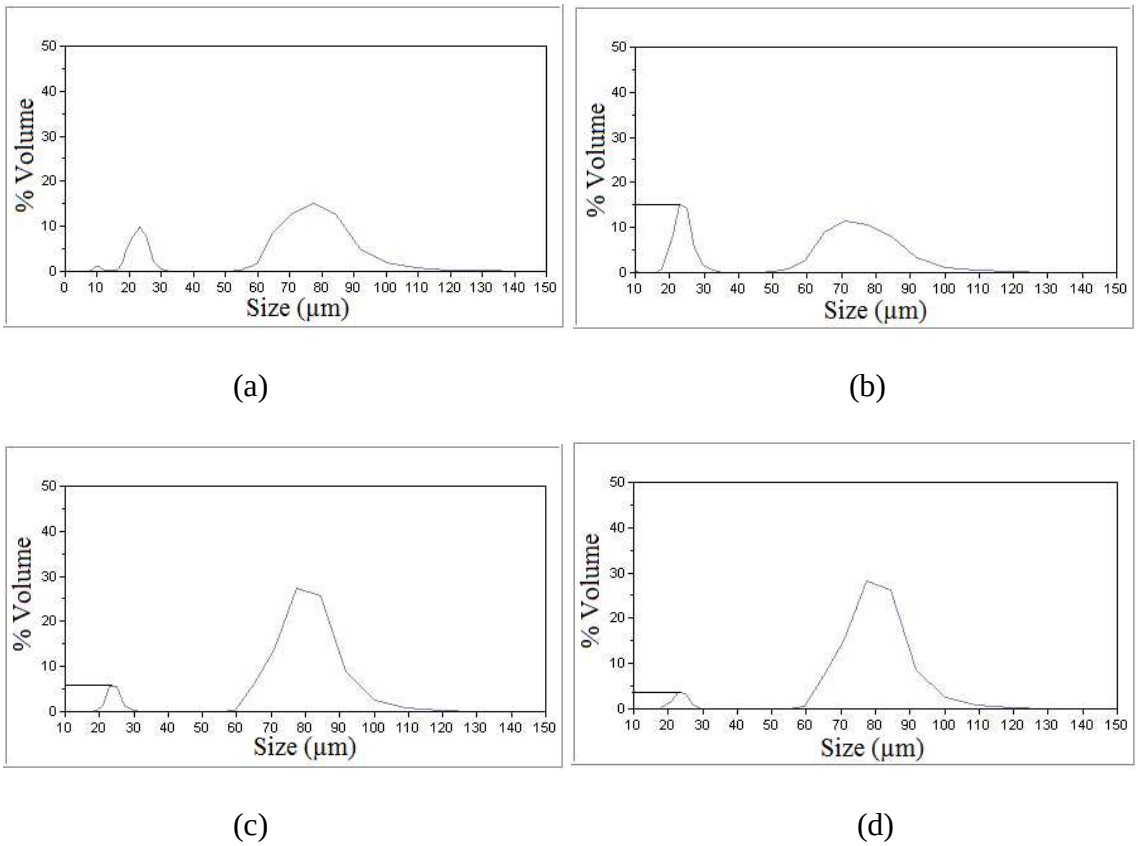

Figure 4.4. Effect of particle feed rate on classifying glass particles (a) PSD of the feed (b) PSD of sample collected from bottom of the system at feed rate 3.2 g/min (c) PSD of bottom sample at feed rate 1.6 g/min (d) PSD of bottom sample at feed rate 0.8 g/min

4.4. EFFECT OF ANNULUS SIZE

The effect of annulus size was studied experimentally by varying the width of the annulus from 1 cm to 2 cm. Soda-lime glass spheres ranging from 10-30 µm were used and Figure 4.5 shows that 10-15 µm particles were not present in the sample collected in the 2 cm annulus, but were present for an annulus size of 1 cm. The maximum amount of particles present in the classified sample also shifts from 20 µm to near 25 µm. This could be attributed to the fact that width of the vortices was increased by doubling the annulus size, leading to an increased number of smaller particles being trapped in the vortices, thereby improving classification. While the data obtained were insufficient to form firm conclusions, further studies with varying annulus sizes need to be performed to observe the effect of annulus size on classification.

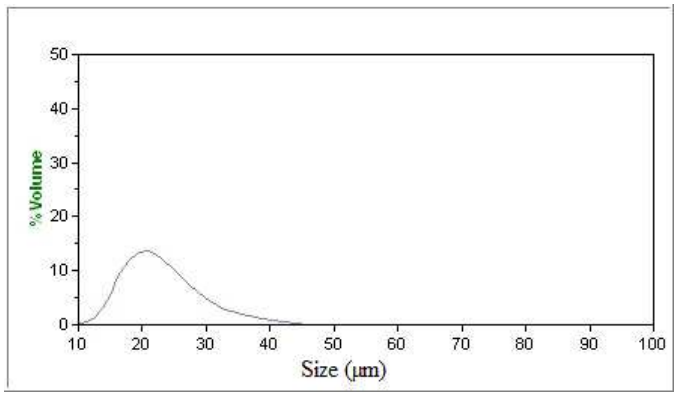

(a)

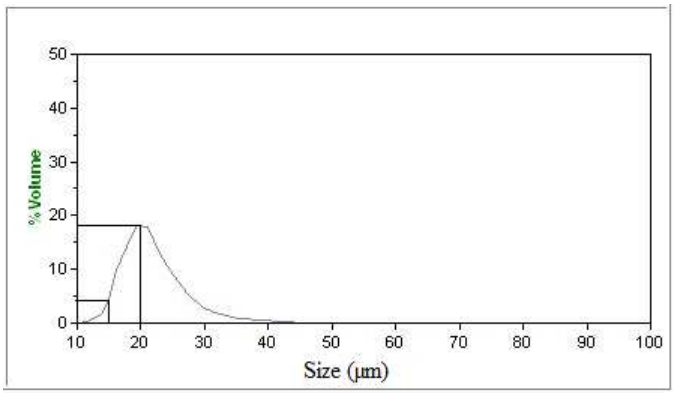

(b)

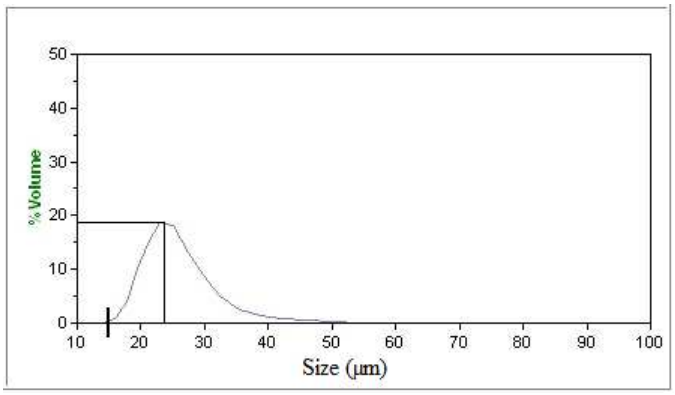

(c)

Figure 4.5. Effect of annulus size on classifying glass particles (a) PSD of feed (b) PSD of bottom sample (1 cm annulus) (c) PSD of bottom sample (2 cm annulus)

4.5. IDENTIFICATION OF CUT-OFF DIAMETER

Cut-off diameter, or cut size (X_{50}), is defined as that value of particle size at which one can expect 50% of those particles to be present in the classified sample [36]. Theoretically, the product sample contains particles whose size is greater than X_{50} and any particle of size less than X_{50} will be absent. However, in real systems, one cannot expect such a sharp cut, so a cumulative value of the population (grade efficiency) of each particle size is taken and the particle size at which grade efficiency is 50% is defined as the cut-size.

Experiments were conducted using 10-30 µm glass particles at different inner cylinder velocities to identify the range of cut-off diameters for the present system. The feed rate of the particles was 0.8 g/min. The results obtained are shown in Figures 4.6 and 4.7. The deviation bars denote the maximum and minimum values obtained during multiple trials. It can be seen from the graph that for the three velocities examined, the cut-off diameter varies from 21.5-25.0 µm as the velocity changes from 35 to 75 rpm. The experimental data obtained (Figure 4.7) for the current system does not show any particular trend. However, further studies at different velocities need to be performed in order to predict the behavior of cut-size with varying velocity. It is expected that cut-size increases with increasing velocity because the presence of smaller particles in the lower third of the system is reduced.

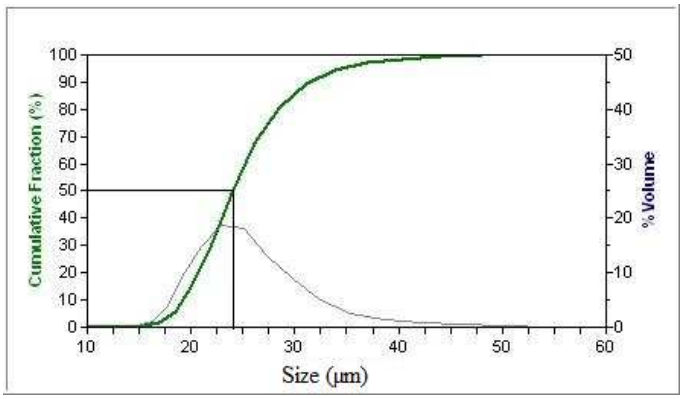

(a)

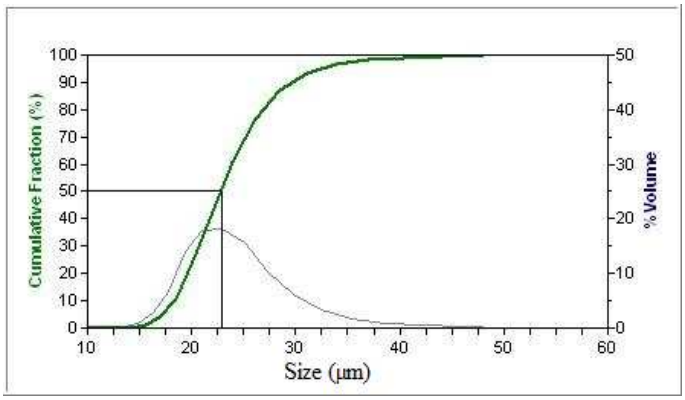

(b)

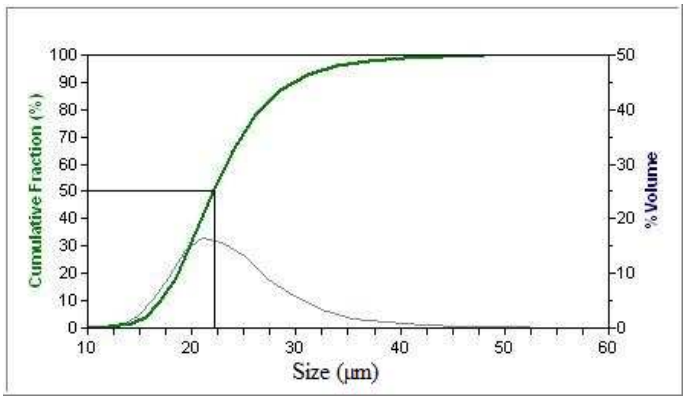

(c)

Figure 4.6. Experimental identification of cut-off diameter for glass particles (single trial): (a) PSD of a sample collected from bottom of the system at 35 rpm (b) PSD of bottom sample at 50 rpm (c) PSD of bottom sample at 75 rpm

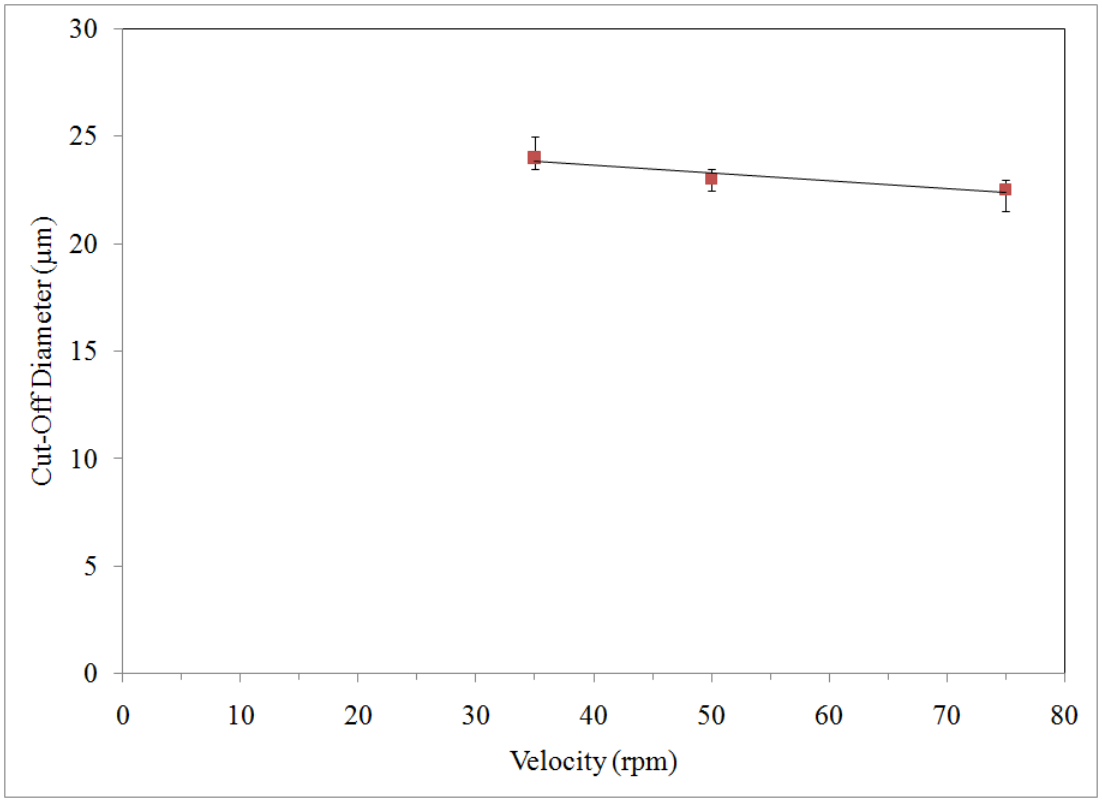

Figure 4.7. Cut-off diameter trends (glass particles)

4.6. NUMERICAL VERIFICATION OF EXPERIMENTAL RESULTS

The experimental values obtained for cut-off diameters did not show any particular trend and were also inconclusive. Since some of the experimental trials showed counterintuitive trends, numerical simulations were conducted for particles of size ranges 10-30 µm and 0.1-10.0 µm to qualitatively verify the experimental trends.

4.6.1. Effect of Inner Cylinder Velocity. It was experimentally predicted that for 10-30 µm particles, a higher amount of separation between the particles was observed at an inner cylinder velocity of 75 rpm than at 35 rpm or 50 rpm. The effect of inner cylinder velocity on classification was studied numerically by varying the inner cylinder velocity from 35 rpm to 75 rpm (Figure 4.8). The feed consisted of equal amounts of 10, 20, and 30 µm glass particles. As seen from Figure 4.8 (a), as the velocity of the inner cylinder increases from 35 rpm to 75 rpm, the percentage of the 10 and 20 µm particles recovered in the lower third of the system decreases, confirming the trend that an increased number of smaller particles are trapped in the vortices with an increase in velocity. A PSD analysis (Figure 4.8 (b)) on the lower third of the system at both 35 rpm and 75 rpm also indicates that the amount of 10 µm particles does not change, while that of 20 µm particles reduces from 34.6% to 28.4% and the relative amount of 30 µm particles in the sample increases from 56.0% to 61.0%. Hence, the amount of 10 µm and 20 µm particles recovered decreases when inner cylinder velocity is raised to 75 rpm, thus validating the trend predicted numerically.

The effect of inner cylinder velocity was also studied numerically for particles 0.18-10.00 µm in size. As seen in Figure 4.8 (c), particles less than 10.00 µm do not follow the expected trend, with the amount of 0.18 µm particles recovered increasing

(rather than decreasing) with increasing velocity and no significant change in the amounts of 3.21 µm and 10.00 µm particles in the lower third of the cylinder. Moreover the difference between the amounts recovered for either the 3.21 µm and 10.00 µm or 0.18 µm and 3.21 µm particles is not large enough to signify separation. This also confirms the experimental prediction that no classification has taken place for particles of this size range within the experimental conditions explored here.

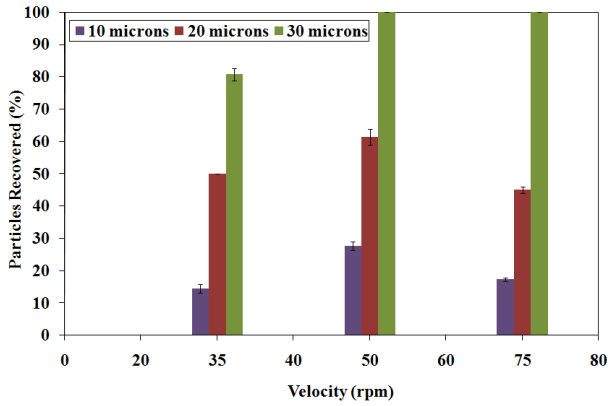

(a)

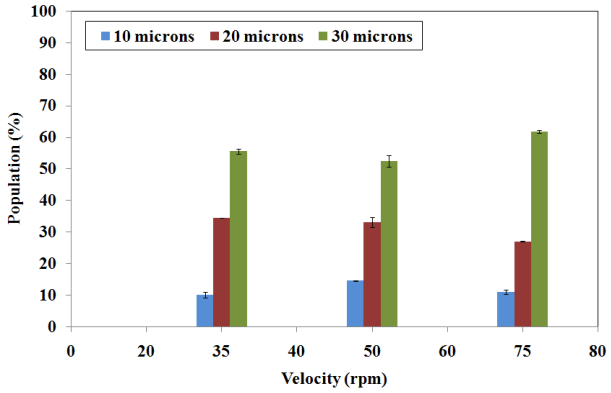

(b)

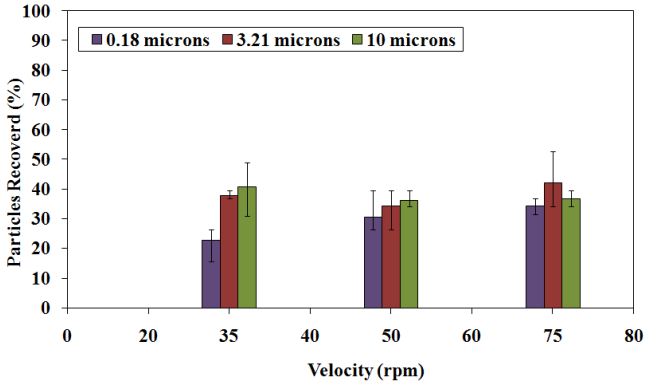

(c)

Figure 4.8. Numerical verification of effect of inner cylinder velocity on classification for glass particles (lower third of the system): (a) Particle recovery for initial size range 10-30 µm (b) PSD for initial size range 10-30 µm (c) Particle recovery for initial size range 0.18-10.00 µm

4.6.2. Identification of Cut-Off Diameter. Cut-off diameter, or cut size (X_{50}), is defined as that value of particle size at which one can expect 50% of those particles to be present in the classified sample [35]. Numerical simulations were conducted using glass particles ranging from 10-30 µm at different inner cylinder velocities to identify whether the value of the cut-off diameter lies between 21.5-25 µm as predicted experimentally. The results obtained are shown in Figure 4.9. It can be seen from the graph that for the three velocities examined, the cut-off diameter varies from 26.5 µm to 29.5 µm. As predicted experimentally, the cut-off diameters did not show any particular trends with varying velocity. Figure 4.10 shows a comparison between the numerical and experimental results obtained.

The cut-off diameters obtained numerically are higher than the experimental predictions. Mechanical vibrations in the experimental system can disturb vortex formation and allow smaller particles to fall to the bottom of the system which could have resulted in the lower values obtained experimentally. Since the numerical system was ideal, and simulations did not take the effects of mechanical vibration into consideration, the numerical results obtained were higher than the values predicted experimentally. Another possible reason for these higher numerical values is that the simulations might not have represented the flow field in the experimental system accurately. This is because even though the numerical system was calibrated, there is a possibility of discrepancy in the results obtained because of the coefficients involved in the turbulent flow equations. The values of the k-ε coefficients used in the simulations were standard and these coefficients might not have been sufficient to accurately model the flow field.

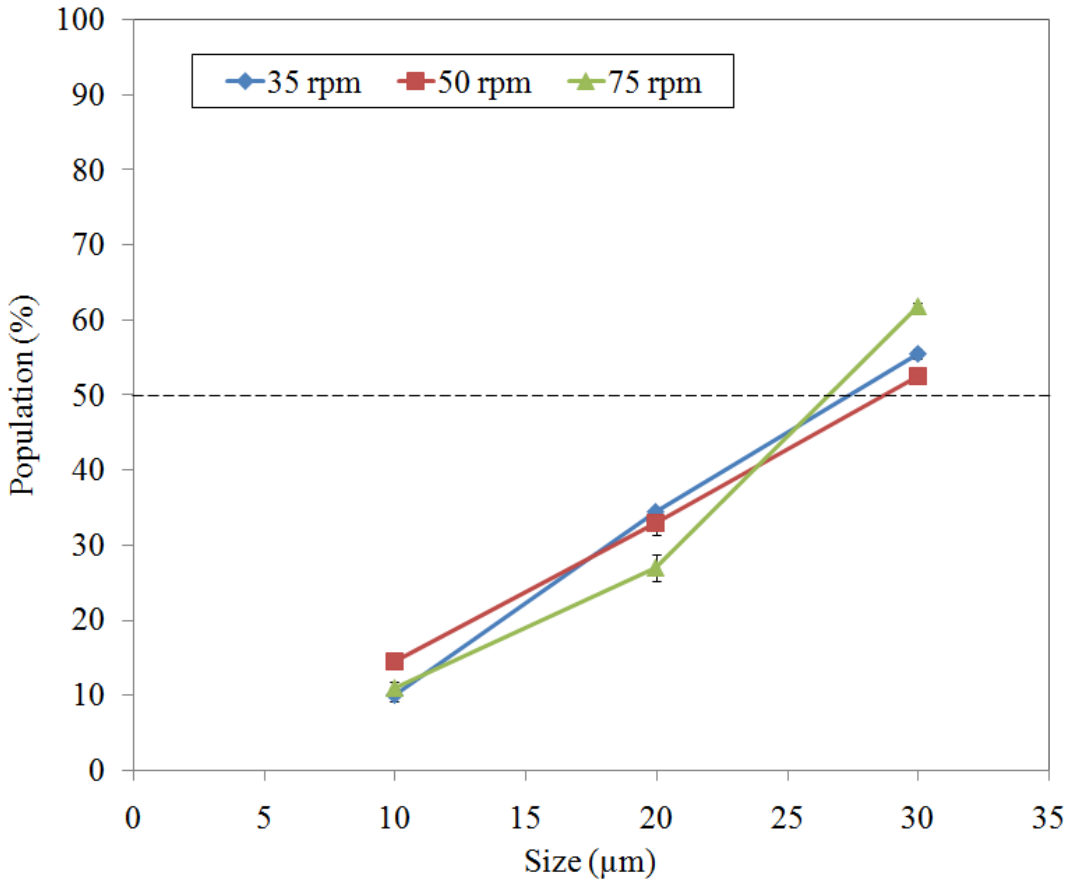

Figure 4.9. PSD of glass particles (lower third of the system) at steady state identifying cut-off diameters

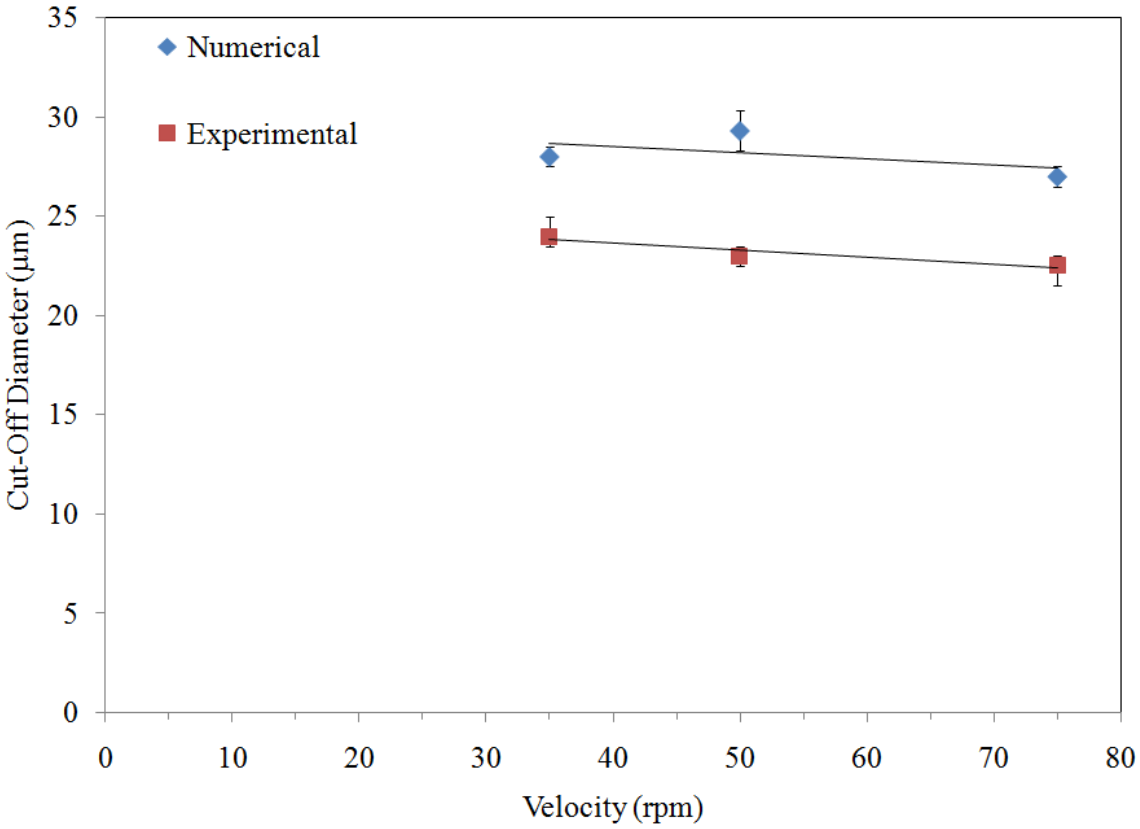

Figure 4.10. Cut-off diameter trends: Experimental and numerical

4.6.3. Effect of Particle to Fluid Density Ratio. Ohmura *et al.* [2] defined factor β as the ratio of particle to fluid density. They verified that classification of fine particles can be achieved for a value of β = 1. However, no study has been performed to verify whether β has any effect on classification. Using glass and nickel particles ranging from 10-30 µm, a numerical study was conducted to study the effect of the ratio of particle to fluid density. In the current numerical study, water was used as the fluid, which led to the values of β being 8.9 and 2.5 for nickel and glass particles, respectively. The results obtained are shown in Figure 4.11. It can be seen from the figure that, at steady state and an inner cylinder velocity of 75 rpm, there is a 10% greater recovery of 20 µm particles at β = 8.9 than at β = 2.5 while no observable difference can be noticed for either 10 or 30 µm particles at these values of β. This leads to the conclusion that the value of β has very little effect on the current system of experimental conditions, though further studies need to be conducted for various other values of β to support the conclusions drawn.

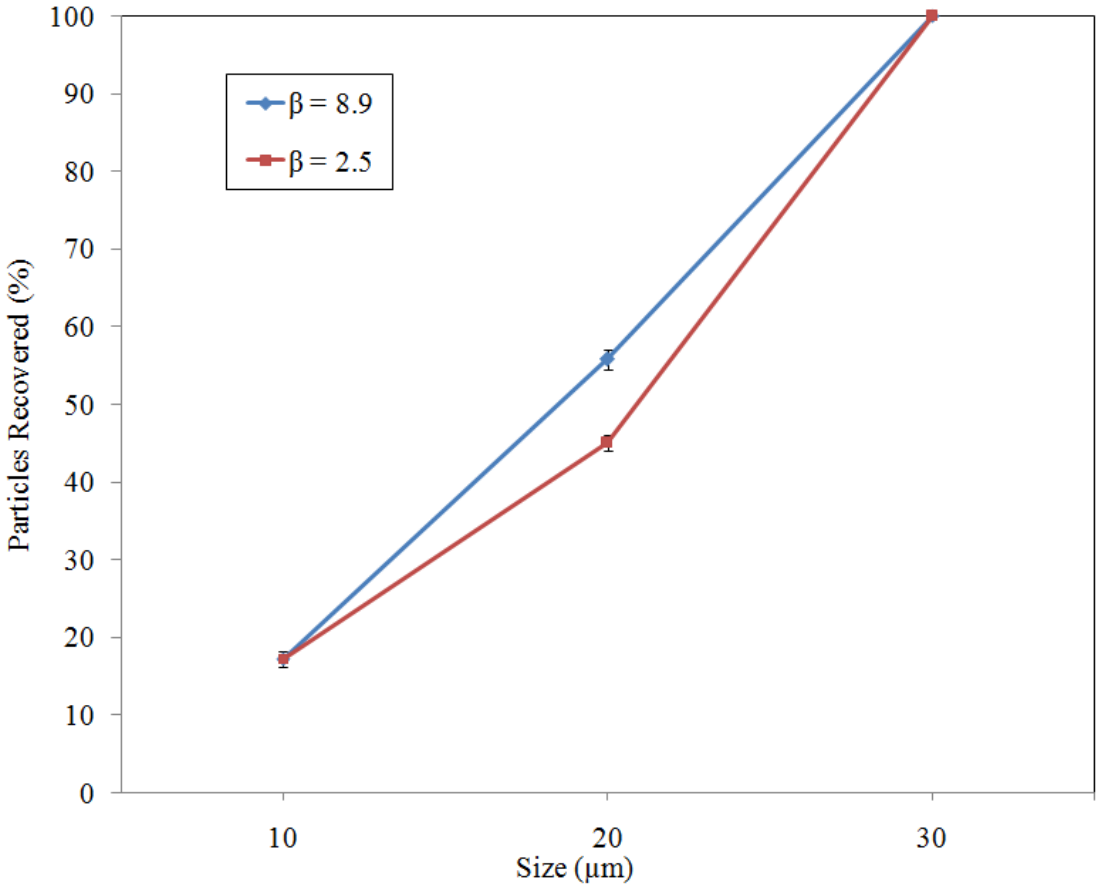

Figure 4.11. Effect of particle to fluid density ratio on classification for glass, nickel particles

5. CONCLUSIONS AND FUTURE WORK

The conclusions that can be drawn from this work are that for the given system and within the ranges studied, inner cylinder velocity, particle feed rate, and annulus size had a significant effect on the classification process and β, the particle to fluid density ratio, did not show much effect. The cut-off diameters for the current system were identified as 26.5-29.5 µm numerically and 21.5-25.0 µm experimentally. Increasing the velocity showed an increased amount of recovery of the 30 µm particles while reducing the amount of 10 µm and 20 µm particles recovered. Lowering the particle feed rate also showed improvement in the classification process with the amount of smaller particles present in a sample obtained from the bottom of the system decreasing from 15% to 4% with a drop in the feed rate from 3.2 g/min to 0.8 g/min.

Doubling the width of the annulus eliminated the presence of smaller particles in the sample obtained from the bottom of the system, indicating that larger annulus leads to better classification, but this must be confirmed by conducting replicate trials of additional experiments with a wider range of annulus sizes. Cut-size of the system did not show any particular trend with varying velocity both numerically and experimentally; however, this must also be confirmed by conducting further experiments with other velocities. The numerical trends of effect of inner cylinder velocity and identification of cut-off diameter compared well with the experimental trends obtained.

Our area of future work would include a study of the effect of system dimensions on the classification process. Some of the preliminary experiments in this direction have shown that with an increment in the annulus size resulting in larger vortices, particle

classification can be improved as larger vortices can trap smaller particles effectively. Varying system height would also be interesting as longer cylinder lengths have been proved to increase the number of vortices [1], potentially leading to better classification as more number of smaller particles would be trapped in the additional vortices formed. Further experiments would also include the verification of the effect of β by varying both fluid and particle material. Ohmura *et al.* [2] have shown that particle classification is possible for β=1 and the present study included the values of β=2.5 and β=8.9. Experiments would be performed by varying either the operating fluid or the material of the particles, for values of β ranging from less than 1 to higher values in order to see if raising or lowering its value would affect the classification process.

Our proposed future work also includes the study of various parameters to achieve classification of particles less than 10 μm in size and also to study the classification process for even narrower distributions consisting of particles with a size difference of 5 μm or less by varying β, annulus size, and inner cylinder velocity. The effect of a wider range of inner cylinder velocities and inlet particle concentrations would also be studied. The effect of lowering inlet particle concentration would be investigated to verify whether or not hindered settling occurs in the process wherein the input concentrations of the particles have been used. This study will help improve the classification efficiency of the Taylor-Couette system.

BIBLIOGRAPHY

[1]. Taylor, G. (1923) "Stability of a viscous liquid contained between two rotating cylinders," *Phil. Trans. R. Soc. London: Series A* 223:289-343.

[2]. Ohmura, N., Suemasu, T., Asamura, Y. (2005) "Particle classification in Taylor vortex flow with an axial flow," *J. Phys.* 14:64-71.

[3]. McCabe, W. (1993) *Unit Operations of Chemical Engineering*, McGraw-Hill Inc., New York.

[4]. Allen, T. (1997) *Particle Size Measurement*, Springer, New York.

[5]. Cooper, D. (1994) *Air Pollution Control – A Design Approach*, Waveland Press Inc, Illinois.

[6]. Geankoplis, C. (2003) *Transport Processes and Separation Process Principles (includes Unit Operations)*, Prentice Hall, New Jersey.

[7]. EPA CICA Fact Sheet – Elutriators, http://www.p2pays.org/ref/10/09869.pdf June 2008

[8]. Pillai, A., Henthorn, K. (2006) "Fine particle classification using fluidized beds in series," *AIChE Conf. Proceedings*, Orlando, April 23-27.

[9]. Davey, A. (1962) "The growth of Taylor vortices in flow between rotating cylinders," *J. Fluid Mech.* 14:336-368.

[10]. http://www.princeton.edu/~gasdyn/Research/T-C_Research_Folder/Intro_to_T-C_Flows.html August 2007

[11]. http://carbon.cudenver.edu/~rtagg/CLARIstyle/CLARIstyle_gifs/Couette_geometry.gif June 2008

[12]. Hodohara, T., Matsumoto, J., Kawahara, M. (2000) "Analysis of the Taylor vortex flow," *International Symposium on Multiphase Flow and Transport Phenomena*, Antalya, Turkey, November 5-10.

[13]. Fox, R., "FLUENT Flow Lab Collaborations – Taylor-Couette flow," http://www.ansys.com/products/flowlab/collaborations/pdfs/taylor_couette_flow.pdf
January 2008

[14]. Ookawara, S., Higashi, R., Street, D, Ogawa, K. (2004) "Numerical study on development of particle concentration profiles in a curved microchannel," *Chem. Eng. J.* 101:171-178.

[15]. Wereley, S., Lueptow, R. (1999) "Inertial particle motion in a Taylor-Couette rotating filter," *Phys. Fluids.* 11:325-333.

[16]. Arifin, D., Smith, K., Deng, R., Wang, C. (2007) "Particle behavior in a Taylor vortex," *AIChE Conf. Proceedings,* Salt Lake City, November 3-9.

[17]. http://www.fluentusers.com/fluent/doc/ori/html/ug/node809.htm
December 2008

[18]. http://www.fluentusers.com/fluent/doc/ori/html/ug/node852.htm
September 2008

[19]. Kuhlmann, H. (1985) "Model for Taylor-Couette flow," *Phys. Rev. Online Archive*, 32:1703-1707

[20]. Broomhead, D., Ryrie, S. (1988) "Particle paths in wavy vortices," *Nonlinearity*, 1:409-434

[21]. Stuart, J. (1986) "Taylor vortex flow: A dynamical system," *SIAM Rev.* 28:10-37

[22]. Chung, T. (2002) *Computational Fluid Dynamics*, Cambridge University Press, New York.

[23]. ANSYS, Inc. White Paper Library, "ANSYS ICEM CFD on Supercomputer helps Designers 'Cut Corners' in Race Car Design," http://www.ansys.com/download-bin/sys-whitepapers.asp
October 2008

[24]. Dhanasekharan, K., Tsai, K., Ring, T., ANSYS, Inc. White Paper Library, "Using Computational Modeling to Control and Optimize the Crystallization Process," http://www.ansys.com/download-bin/sys-whitepapers.asp
October 2008

[25]. Bird, R., Stewart, W., Lightfoot, E. (2002) *Transport Phenomena*, Wiley, New York.

[26]. Date, A. (2005) *Introduction to Computational Fluid Dynamics*, Cambridge University Press, New York.

[27]. Wesseling, P. (2001) *Principles of Computational Fluid Dynamics*, Springer, New York.

[28]. Petrila, T. (2005) *Basics of Fluid Mechanics and Introduction to Computational Fluid Dynamics*, Springer, New York.

[29]. Shyy, W., Rao, M., Smith, R., Udaykumar, H. (1996) *Computational Fluid Dynamics with Moving Boundaries*, Taylor & Francis, Washington.

[30]. Ferziger, J., Peric, M. (2002) *Computational Methods for Fluid Dynamics*, Springer, New York.

[31]. Davidson, P. (2004) *Turbulence: An Introduction for Scientists and Engineers*, Oxford University Press, New York.

[32]. Wilcox, D. (2006) *Turbulence Modeling for CFD*, DCW Industries Inc., California.

[33]. Wereley, S., Lueptow, R. (1998) "Spatio-temporal character of non-wavy and wavy Taylor-Couette flow," *J. Fluid Mech.* 364:59-80.

[34]. Stuecke, P., Lehmann, B., Scurtu, N., Egbers, C. (2008) "Experimental investigation of the eccentric Couette flow with superimposed cross flow," *J. Phys.: Conf. Ser.* 137 012010.

[35]. http://www.fluentusers.com/fluent/doc/ori/html/ug/node477.htm December 2008

[36]. Rhodes, M. (1998) *Introduction to Particle Technology*, John Wiley, New York.

VITA

Navina Durgaiah Tungapindi was born on April 8, 1985 to Vidyadhari and Durgaiah Tungapindi at Hyderabad, India. She completed her Bachelor of Technology in Chemical Engineering from Osmania University in June 2006. She joined Missouri University of Science & Technology in Fall 2006 for Master of Science in Chemical Engineering and will receive her degree in May 2009.